Title

Enhancing Tumor-Infiltrating T cells with an Exclusive Fuel Source

Author

Miller, Matthew Lawrence

Publication Date

2024

Peer reviewed|Thesis/dissertation

UNIVERSITY OF CALIFORNIA

Los Angeles

Enhancing Tumor-Infiltrating T cells with an Exclusive Fuel Source

A dissertation submitted in partial satisfaction of the

requirements for the degree Doctor of Philosophy

in Molecular Biology

by

Matthew Miller

2024

ABSTRACT OF THE DISSERTATION

Enhancing Tumor-Infiltrating T cells with an Exclusive Fuel Source

by

Matthew Miller

Doctor of Philosophy in Molecular Biology

University of California, Los Angeles, 2024

Professor Manish J. Butte, Chair

Solid tumors harbor immunosuppressive microenvironments that inhibit tumor-infiltrating lymphocytes (TILs) through the voracious consumption of glucose. We sought to restore TIL function by providing them with an exclusive fuel source. The glucose disaccharide cellobiose, which is a building block of cellulose, contains a β-1,4-glycosidic bond that cannot be hydrolyzed by animals (or their tumors), but fungal and bacterial organisms have evolved enzymes to catabolize cellobiose and use the resulting glucose. By equipping T cells with two proteins that enable import and hydrolysis of cellobiose, we demonstrate that supplementation of cellobiose during glucose withdrawal restores T cell cytokine production and cellular proliferation. Murine tumor growth is suppressed, and survival is prolonged. Offering exclusive access to a natural disaccharide is a new tool that augments cancer immunotherapies. Beyond cancer, this approach could be used to answer questions about the regulation of glucose metabolism across many cell types, biological processes, and diseases.

The dissertation of Matthew Miller is approved.

Steven J. Bensinger

Heather R. Christofk

Robert M. Prins

Orian Shirihai

Manish J. Butte, Committee Chair

University of California, Los Angeles

2024

DEDICATION

I am very grateful to a host of people for their support before and during the years it took me to complete this work; it takes a village. There are a few people I would like to highlight:

To my parents, John and Martha – without your enduring support, this work would not have been possible; I am standing on your shoulders. Thank you for being there to celebrate with me in the best of times, and for propping me up through life's toughest moments.

To my life-partner (and future wife), Ana – you are my role model and make each day so fulfilling. Embarking on this journey with you has been a privilege beyond measure. Thank you for your patience and wisdom.

To my mentor, Manish – my integrity as a scientist has been profoundly impacted by your guidance. Your zeal for knowledge and impact was a constant boon through this challenging time. I doubt this project could have been explored in many other settings; thank you for believing in me.

TABLE OF CONTENTS

LIST OF FIGURES

LIST OF ACRONYMS

APC – antigen-presenting cell

CAR – chimeric antigen receptor

CDT-1 – cellodextrin transporter 1, cellobiose transport protein

CG-T cells – CDT-1 GH1-1 T cells; T cells coexpressing CDT-1 and GH1-1

CTV – CellTrace Violet

ECAR – extracellular acidification rate

EL4-OVA – T lymphoblast cancer cells/tumors expressing ovalbumin protein

GAPDH – glyceraldehyde 3-phosphate dehydrogenase

GFP – green fluorescent protein

GH1-1 – glycosylhydrolase family 1-1, cellobiose hydrolase enzyme

GOI – gene of interest

HIF1a – hypoxia-inducible factor 1-alpha

HK2 – hexokinase II

IFNg – interferon-γ

IL-2 – interleukin-2

LC-MS – liquid chromatography-mass spectrometry

LDHA – lactate dehydrogenase A

mCherry – red fluorescent protein

MFI – mean fluorescent intensity

MHC – major histocompatibility complex

OT-I – T cell receptor that binds ovalbumin peptide residues 257-264 ($OVA_{257-264}$) in the context of $H2K^b$ MHC

PBS – phosphate-buffered saline

PDH – pyruvate dehydrogenase

PD-L1 – programmed death-ligand 1

PD-1 – programmed cell death protein 1

TCA – tricarboxylic acid

TCR – T-cell receptor

TIL – tumor-infiltrating lymphocyte

TME – tumor microenvironment

TNF – tumor necrosis factor

VEGF – vascular endothelial growth factor

ACKNOWLEDGEMENTS

Chapter 4 is a version of:

ML Miller, R Nagarajan, TJ Thauland, MJ Butte. Enhancing Tumor-Infiltrating T cells with an Exclusive Fuel Source. 2024. *Submitted*.

Rina Nagarajan provided day-to-day support and independently conducted experiments and data acquisition that appear in the final manuscript.

Timothy J. Thauland provided hands-on expertise and assistance with assays, technical support, and guidance in experimental design.

Manish J. Butte was the principal investigator and provided guidance in experimental design. He helped to write and edit the final manuscript.

CURRICULUM VITAE

Education

University of California, Los Angeles [2017 - present]
Molecular Biology Interdepartmental Doctoral Program

University of California, Berkeley [2009 - 2013]
BS Molecular Environmental Biology

Research Experience

UC Los Angeles, Lab of Manish J. Butte, MD, PhD
Graduate Student Researcher [2018 - present]
Research projects centered around cancer immunotherapy, metabolic pathways, protein engineering, and gene editing.

- Engineered T cells to enable use of a novel fuel source during tumor infiltration
- Developed a gene-marking strategy to enrich genetically modified stem cells
- Secured ~$350,000 in funding through multiple grants and awards
- Mentored 5+ graduate, undergraduate, high school students, technicians

UC San Francisco, Lab of William A. Weiss, MD, PhD
Volunteer, Staff Research Associate I, Staff Research Associate II [2014-2017]
Led a genome editing project, mentored a full-time volunteer, served as interim lab manager, and carried out day-to-day tasks for my mentor.

- Developed CRISPR systems to generate large chromosomal deletions in stem cells
- Performed renal capsule and intracranial surgeries in mice for orthotopic cell injection
- Differentiated pluripotent stem cells (iPSC/hESC) into neural crest stem cell lineages
- Cloned a large variety of genetic constructs into Piggybac and lentiviral vectors

UC Berkeley, Lab of Cèline Pallud, PhD
Research Assistant [2012 - 2013]

Peer-Reviewed Publications

Miller ML, et al. Enhancing Tumor Infiltrating T cells with an Exclusive Fuel Source. **Submitted.** September 2023.

Hasani-Sadrabadi MM, et al. Augmenting T-cell responses to tumors by *in situ* nanomanufacturing. **Material Horizons**. 2020 Sept; 7, 3028-3033.

Huang M, et al. Engineering Genetic Predisposition in Human Neuroepithelial Stem Cells Recapitulates Medulloblastoma Tumorigenesis. **Cell Stem Cell.** 2019 Sept 5; 25:1–14.

Parker BL, et al. An integrative systems genetic analysis of mammalian lipid metabolism. **Nature.** 2019 Feb 27; 567:187-193..

Huang M, et al. Generating trunk neural crest from human pluripotent stem cells. **Scientific Reports.** 2016 Jan 27; 6:19727.

Leadership and Mentoring

America Needs You (ANY), Mentor Coach [2019 - 2020]

Student Research Program (SRP-199), Graduate Student Mentor [2018 - 2020]
Letters to a Pre-Scientist, Pen-Pal [2018 - 2020]
Entering Mentoring Training Program, Alumni [Spring 2019]

Awards and Honors

Metabolism in Health in Disease Conference (Fusion), Best Poster Award [May 2022]
Johnson Comprehensive Cancer Center Retreat (UCLA), Best Poster Award [May 2022]
SACNAS, Member of the Quarter [Fall 2018]

Teaching

UCLA, **BISEP, Biomedical Sciences Enrichment Program** – Lab Leader [Summer, 2022]
UCLA, **MCD BIO M140, Cancer Cell Biology** – Teaching Assistant [2019, 2020]
UCLA, **Entering Mentoring Training Program** – Alumni [Spring 2019]
UCLA, **LIFESCI 495, Teaching in Life Sciences** – Student [Winter 2019]

Conference Abstracts

Miller, ML, Butte MJ. Immunoengineering an exclusive fuel source to enhance tumor infiltrating lymphocytes. UCLA Cancer Symposium 2022 (Los Angeles, CA, USA)

Miller, ML, Butte, MJ. Engineering an exclusive fuel source to enhance tumor infiltrating T cells. Fusion Metabolism Conference 2022 (Cancun, Mexico)

Huang M, et al. Human pluripotent stem cell-based models of MYCN-amplified neuroblastoma. Advances in Neuroblastoma Research Conference 2016 (Cairns, Australia)

Huang M, et al. Human stem cell-based model of medulloblastoma derived from Gorlin syndrome iPSC (poster), ISSCR/CIRA International Symposium 2016 (Kyoto, Japan)

Huang M, et al. Modelling neuroblastoma-related chromosome deletions in human stem cells. Keystone Symposium on Precision Genome Engineering and Synthetic Biology 2015 (Big Sky, Montana)

Talks

Immunology, Infection, Inflammation, and Transplantation (I3T) Seminar [April 2021]

Funding

NIAID – R21 – Exploratory/Developmental Grant [Summer 2022]
NIH – T32 – Cellular and Molecular Biology Training Program [2019 - 2021]
Johnson Comprehensive Cancer Center Fellowship Award [August 2021]

Patents

Methods and Agents for Modulating Immunotherapy*, U.S. Provisional Application* – 63/173, 133, March 2021

Societies and Associations

Member, American Association for the Advancement of Science (AAAS) [2017 - present]
Member, SACNAS [2018 – 2021]

CHAPTER 1

METABOLIC PERTURBATION IN SOLID TUMORS

1a. Mutations Make Metabolic Cheaters

Coordination within multicellular organisms is of critical importance for their survival, growth, and reproduction. As these organisms are composed of diverse cell types, each with specialized functions, the seamless integration of their activities ensures the organism operates as a cohesive unit. Without this intricate coordination, vital processes such as nutrient absorption, waste elimination, and response to environmental stimuli would become disjointed, potentially leading to systemic failures. The ability of different cell types to communicate and work together provides multicellular organisms with the flexibility to adapt to changing conditions and perform complex tasks that individual cells alone could not accomplish. In essence, coordination is the cornerstone of complexity in multicellular life, enabling higher-order functions and fostering evolutionary advantages.

Within multicellular organisms, "cheater" cells are those that deviate from the collective norms, gaining advantages at the expense of other cells[1]. Instead of cooperating and fulfilling their specialized roles, these cells can exploit the system, consuming resources or avoiding programmed cell death, often leading to detrimental effects on the organism as a whole. A prime example of such behavior can be seen in cancer. Cancerous cells divide uncontrollably, siphoning off nutrients and space, and can evade the body's regulatory mechanisms meant to curtail their growth. By doing so, they compromise the integrity and functioning of the surrounding tissues. The emergence of cheater cells underscores the delicate balance required in multicellular systems, where individual cell behavior must be harmonized for the overall health and survival of the organism.

Cancer cells "cheat" largely due to mutations that accumulate within their DNA, disrupting the usual checks and balances that regulate cellular behavior[2]. In healthy cells, a complex interplay of signals governs processes like cell division, differentiation, and apoptosis (programmed cell death). However, when mutations occur in genes responsible for these

regulatory processes, a cell may begin to evade these controls. For example, mutations in oncogenes can drive uncontrolled cell division, while mutations in tumor suppressor genes can disable the cell's ability to undergo apoptosis when damaged. As these rogue cells proliferate, they prioritize their own growth and survival over the well-being of the organism, consuming disproportionate resources and often disrupting the normal function of tissues and organs. Ultimately, the DNA mutations result in an unchecked advantage that allows cancer cells to proliferate, creating masses or tumors that ultimately endanger the host organism.

Many of the most commonly occurring mutations in cancer directly impact cellular metabolism by altering nutrient uptake and processing. The tumor suppressor gene, *TP53*, is the most frequently mutated gene in human cancers (mutated in 35% of all cancers)[3] and was initially identified for its role in repairing DNA damage and inducing apoptosis in genetically damaged cells. More recent work, however, has identified a role for the p53 protein in modulating metabolism. Mutations in *TP53*, the gene that encodes p53, can directly promote the expression of the glucose transporters GLUT1 and GLUT4[4], up-regulate phosphoglycerate mutase (PGM) activity[5], and inhibit TIGAR (TP53-induced glycolysis and apoptosis regulator) activity[6]. The net result of these modified behaviors is an increased uptake of glucose from the extracellular environment followed by elevated flux through the glycolytic pathway. The increased consumption of glucose occurs at the cell intrinsic level, without external cues to do so, leading cancerous cells to siphon off this nutrient from the extracellular environment irrespective of negative feedback that might normally curb this process.

Cancer cells can also harbor mutations that, in the absence of extracellular cues like growth hormones or nutrient rich environments, result in constitutive growth and/or division programs. Transforming mutations in *EGFR, KRAS, BRAF,* and *PIK3CA* are prevalent in cancer[3] and can result in downstream activation of cellular programs that promote survival, growth, and proliferation. These functions are energy and resource intensive and ultimately depend on a

rewiring of metabolic machinery to support anabolic pathways that build lipids, proteins, and nucleic acids. As the cell reorganizes the metabolic networks that facilitate the production of these macromolecules, it begins to pull in high quantities of energy rich molecules from the extracellular environment, including glucose and glutamine.

It was nearly a century ago that physician Otto Warburg first observed this metabolic reorganization in cancer cells. He noticed that, unlike healthy tissue, cancerous tissue consumed abnormally large quantities of glucose and displayed elevated rates of glycolysis[7]. Up to that point, microbes were well-known to exhibit a high glycolysis phenotype, which was primarily seen in anaerobic contexts[8]. In contrast, Warburg showed that cancerous tissue exhibited elevated glucose consumption rates and increased production of lactate, even when oxygen was abundantly available. He coined this phenomenon as “aerobic glycolysis”, or glycolysis that occurs despite the presence of sufficient oxygen to satisfy mitochondrial respiration. Since then, aerobic glycolysis has been observed in and is associated with highly proliferative tissues. Aerobic glycolysis is so commonplace among cancer that it has led to decades of speculation and scientific debate regarding the function of glycolysis in rapidly dividing cells.

1b. Glucose is a Keystone Nutrient

Glycolysis, or the step-wise breakdown of glucose, is an ancient pathway and evolved in unicellular organisms before oxygen was abundant in the environment[9]. Glucose is a major source of cellular energy and biomass, and accounts for approximately half the caloric intake in humans[10]. In human metabolism, glucose has long been viewed as a source of pyruvate (Wikipedia describes glycolysis as "the metabolic pathway that converts glucose into pyruvate"[11]), but recent insights have enriched our understanding of the multifaceted functions of glycolysis. From an energetic perspective, pyruvate is indeed a critically important compound because it may pass into the mitochondrial matrix, where the pyruvate dehydrogenase (PDH) complex catalyzes its conversion into acetyl-CoA. Acetyl-CoA is an essential component of the tricarboxylic acid (TCA) cycle, where oxidative phosphorylation facilitates the transfer of electrons off the acetyl carbons and into the mitochondrial electron transport chain, a process that ultimately yields significant quantities of ATP.

While the passage of glucose carbons into the TCA cycle via pyruvate is undoubtedly an important function of glucose catabolism, the elevated rate of glucose consumption in highly proliferative cells (including cancer) cannot be explained solely by the need to generate more pyruvate for more energy production, a notion that is supported by multiple observations. First, ATP is not a limiting factor for cell growth and proliferation[12]. In fact, the rate-limiting step of glycolysis (catalyzed by phosphofructokinase) is restrained by ATP consumption rather than its production[13,14]. Second, transcription factors like *MYC* and *HIF1A*, which strongly upregulate glycolysis and are known to be master regulators and promoters of growth and proliferation programs, strongly upregulate the expression of pyruvate dehydrogenase kinase 1 (PDK1) and lactate dehydrogenase A (LDHA)[15–17]. Both PDK1 and LDHA serve to direct pyruvate away from mitochondrial oxidation, by inhibiting the conversion of pyruvate into acetyl-CoA and catalyzing the reduction of pyruvate into lactate, respectively. In fact, in highly proliferative cells, roughly 90%

of glucose carbons are converted into lactate or alanine, suggesting that less than 10% of pyruvate is oxidized in the TCA cycle[18]. These observations indicate that there are needs beyond yielding ATP that explain the increased consumption of glucose in highly proliferative cells.

When a cell divides, it must duplicate all cellular contents, including proteins, lipids, DNA, and RNA. Recent work has refined our understanding of the role of glycolysis, where glucose catabolism plays a crucial role in the anabolic processes that underpin cell division. Glucose serves not just as an energy source, but perhaps even more vitally, as a precursor for many of the amino acids, nucleic acids, and lipids that are built into the macromolecules that ultimately compose the cell. Glucose carbons not only flow down the “standard” glycolytic pathway, but also into ancillary pathways that efficiently construct these fundamental building blocks.

The pentose phosphate pathway is a major offshoot of glycolysis and generates the nucleotides that serve as the fundamental building blocks of DNA and RNA. Nucleotides compose a significant portion of cell mass, estimated to be roughly ~25% of total dry weight in *E.* coli[19]. Purines (e.g. ATP, dATP, GTP, and dGTP) and pyrimidines (e.g. CTP, dCTP, UTP, and dTTP) are nucleotides primarily built from the acquisition of glucose carbons[20]. For example, out of the 10 carbons found in purines, glucose contributes to a minimum of five and a maximum of nine of these carbons[21]. A high rate of glucose catabolism is required to generate the necessary precursor pool to support nucleotide synthesis during cell division. As glucose catabolism ramps up after mitogenic stimulation, PRPP synthetase, which catalyzes a rate-limiting reaction in purine synthesis, also increases in expression[22]. The parallel increase in glucose consumption and PRPP synthetase expression seen in rapidly dividing cells, and the loss of nucleotide synthesis when glycolysis is blocked, suggests an important role for glucose in generating precursors of nucleotide synthesis.

Proteins represent the bulk of cellular content, accounting for roughly ~50% of dry cell mass in mammalian cells[23]. The high protein content imposes a significant burden for proliferating cells to generate enough amino acids to support protein synthesis. Out of the 11 non-essential amino acids (i.e. those that are not strictly acquired through diet), glycolytic metabolites can make direct contributions to the synthesis of four of them. Pyruvate can be directly converted into alanine, while another glycolytic intermediate, 3-phosphoglycerate, can provide the carbons for serine, glycine, and cysteine. The availability of free amino acids largely influences the activities of the signal transduction complexes mTORC1 and mTORC2, which are responsible for sensing environmental nutrient conditions (including glucose abundance[24]) and coordinating those inputs with cellular growth activities. Therefore, highly proliferative cells depend on glucose to generate several of the amino acids that are used in protein biosynthesis and that engage the signal transduction complexes that sustain growth programs.

Beyond glucose catabolites serving as direct precursors for de novo assembly of nucleotides and proteins, glucose is also an important carbon source in the construction of lipids, which represent some ~10% of cell mass[19]. Glucose carbons that are transported into the mitochondrial matrix as pyruvate and converted into acetyl-CoA can still be diverted away from energy production and instead be recycled to augment lipogenesis. After acetyl-CoA enters the mitochondrial TCA cycle and combines with oxaloacetate to form citrate, excess citrate may be exported from the mitochondria, where the enzyme ATP citrate lyase regenerates acetyl-CoA. Cytosolic acetyl-CoA can then participate in the synthesis of fatty acids and sterols[25]. Serine, a glucose derived amino acid, is also an important carbon source in lipid biosynthetic reactions. Serine may serve as a precursor for ethanolamine and choline, which serve as head groups for some phospholipids, or may be used to modify a glycerol headgroup to generate phosphatidylserine, an abundant and functionally important component of the cell membrane.

While the role of aerobic glycolysis in rapidly proliferating cells may primarily serve to increase short-term energy needs and to increase the precursors that are available for biosynthesis, it may seem confounding that this process leads to such a high fraction of the glucose carbons being expelled as lactate. In cultured glioblastoma cells undergoing aerobic glycolysis, roughly 90% of glucose carbons end up as lactate or alanine[18] , a high fraction of which is then excreted from the cell. The answer may involve the relative fluxes of glycolysis and the ancillary pathways being fed by glycolytic catabolites. A low-flux pathway (biosynthetic) would be highly sensitive to the rate of the pathway from which the inputs are derived (glycolysis)[26]. When glycolytic rates are high, biosynthesis can efficiently occur, but if glycolytic rates diminish, the rate of biosynthesis would quickly come to a halt. Therefore, the high flux of glucose to lactate may be a means of regulating biomass production, allowing increased biosynthesis to occur only when abundant environmental resources are sensed and fluxing through the cell. Another rationale for the high fraction of glucose carbons that end up as lactate involves the redox state of the cytosolic compartment. The accumulation of reduced NAD (NADH) would result in a diminished abundance of electron acceptors, which inhibits glycolytic turnover. Pyruvate reduction into lactate allows for oxidized NAD (NAD+) to be regenerated, allowing for recycled use in upstream glycolytic reactions and enabling glycolysis to continue at a high rate.

Glucose also plays an important functional role in the cell through the modification of macromolecules. Upon entering the cell, glucose is immediately phosphorylated by hexokinase II (HK2) to generate glucose-6-phosphate. This metabolite may traverse the standard glycolytic pathway or may undergo isomerization to glucose-1-phosphate before conversion into UDP-glucose. In cells that accumulate energy reserves (e.g. adipocytes), UDP-glucose plays a significant role in regulating the balance of intracellular glycogen levels. UDP-glucose can also donate the reduced glucose group to lipids and proteins and modify their function. For example, the enzyme UDP-glucose ceramide glucosyltransferase catalyzes the transfer of glucose from

UDP-glucose to a ceramide, generating a glycosphingolipid, which is an essential member of the cell membrane that participates in a milieu of cellular functions[27]. Another glucosyltransferase, UDP-glucose:glycoprotein glucosyltransferase, plays an important role in glycoprotein folding control by transferring glucose from UDP-glucose to nascent polypeptides, which influences the ability of the polypeptide to interact with chaperon proteins, and ultimately allows them to fold correctly and carry out their functions[28]. UDP-glucose can also be processed into UDP N-acetylglucosamine (UDP-GlcNAc), a metabolite used by glycosyltransferases to transfer N-acetylglucosamine (GlcNAc) to a wide variety of proteins. Post-translational modifications with GlcNAc are implicated in a vast number of biological processes by influencing the water solubility of macromolecules, physical expulsion of pathogens, diffusion barriers, protection from proteases, membrane organization, protection from immune recognition, and epigenetic histone modifications[29].

1c. Depleted Glucose Availability in the Solid Tumor Environment

In cells that are transcriptionally wired for growth and proliferation, the essential and central role of glucose in cellular biosynthesis and function results in a high rate of glucose consumption. To support continual glycolytic flux and enable the efficient import of glucose, the expression of glucose transporters (e.g. GLUT1, GLUT3, and GLUT4) is commonly upregulated in proliferative cells[30,31]. These transporters facilitate diffusion of glucose down a concentration gradient, from high concentrations in the extracellular space to relatively lower concentrations in the intracellular space. Once inside the cell, glucose is rapidly phosphorylated by HK2, preventing efflux back out of the cell through the same glucose transporters through which it arrived. Phosphorylation by HK2 also reduces the concentration of glucose in the cell, allowing the glucose concentration gradient to remain lower inside the cell relative to the extracellular space, further enabling unidirectional flow[32]. The high levels of glucose transporters present at the plasma membrane and the immediate phosphorylation of glucose once inside the cell enable a constant and steady inward flow of glucose to support the elevated rates of glycolysis found in rapidly dividing cells.

In healthy tissue, extensive capillary networks enable a continuous supply of glucose and oxygen to support both basal metabolic needs as well as the heightened modes of metabolism found in proliferative tissues. The structure of these capillary beds is highly organized and ensures a minimal diffusion distance for resources delivered from major arteries. If cells divide to the extent that they are a significant distance from capillary diffusion, oxygen tension diminishes, allowing for stabilization of hypoxia inducible factor 1-alpha (HIF1a), a master transcriptional regulator of multiple gene networks that enable cells to cope with hypoxic challenge[33,34]. As part of these transcriptional programs, vascular endothelial growth factors (VEGF) are induced, a family of signaling proteins that potently stimulate the production of new blood vessels. The circuit between diminished oxygen supply, increased HIF1a activity, and new blood vessel formation is essential

to ensure that proliferative tissues receive adequate nutrient and oxygen supply, which ultimately allow for the continued engagement of the anabolic modes of metabolism that underly cell growth and division.

Beyond induction of angiogenesis, HIF1a also directly modulates metabolism by promoting glycolysis and downregulating mitochondrial output, with the net change allowing for metabolic function to persist in hypoxic environments. HIF1a increases extracellular uptake of glucose by directly inducing expression of glucose transporters[35], as well as by promoting the translocation of glucose receptors from intracellular vesicles to the plasma membrane[36]. HIF1a also directly or indirectly induces *all* of the genes involved in the core glycolytic pathway, that is from the conversion of glucose to pyruvate[37]. LDHA, the enzyme responsible for regenerating NAD+ in cells with high glycolytic flux, and monocarboxylate transporter 4 (MCT4), the transporter responsible for lactate efflux, are also induced by HIF1a[38,39]. As HIF1a promotes transcription of glycolytic genes, it concurrently inhibits mitochondrial output. PDK1, a protein responsible for inhibiting the flow of pyruvate into the mitochondria and thus reducing mitochondrial redox potential, is a direct transcriptional target of HIF1a[40,41].

Glucose metabolism is dynamically regulated and responsive to a host of environmental factors, including nutrient availability and oxygen tension. Cancer cells operate in a different environmental context, devoid of proper tissue architecture. While cancerous tissues often secrete VEGF to generate new vasculature and sustain growth, most tumors fail to produce sufficient levels of angiopoietin proteins, growth factors that are essential for the maturation of blood vessels[42,43]. The absence of angiopoietin during angiogenesis results in fewer cell-cell junctions[44], defective pericyte coverage[45], and patchy basement membranes[46]. Ultimately, tumor vasculature networks lack the structural hierarchy of normal vascular beds, resulting in disorganized and dysfunctional vessels that produce perturbed, arbitrary blood flow, leading to

large sections of tumors being poorly perfused. The sluggish blood flow results in hypoxic zones, the induction of HIF1a, and the upregulation of glycolysis.

Beyond generating abnormal tissue architectures, cancer cells do not respond to environmental feedback in the same manner as healthy tissue. When proliferative and hypoxic cells continuously consume glucose, it may begin to deplete from the tumor environment. Healthy cells are capable of sensing the environmental challenge of nutrient depletion, through nutrient and energy sensors along the mTOR-AMPK axis[47–50], resulting in a curtailment of metabolic and proliferative activity. Cancer cells harbor genetic mutations that hardwire cell cycling and increased metabolism, including many upstream of mTOR[3]. As a result, cancer cells continuously engage elevated metabolic flux through the glycolytic pathway, regardless of the nutrient context of their environment.

Blood glucose concentration is relatively stable in healthy humans and mice, ranging between 4-8 mM depending on whether the measurement is taken during a fed or fasted state[51,52]. The concentration of glucose in the interstitial fluid of well-perfused tissues can approach the concentration found in blood[53], but may decline in tissues with less extensive vascularization. As glucose is continuously consumed by insatiable cancer cells, the glucose concentration within tumor tissue becomes appreciably anomalous to healthy tissue. Mass spectrometry-based profiling of human stomach and colon cancers determined the concentration of glucose to be 13 and 45 times less than blood, respectively, and 3 and 10 times less than the concentration found in healthy, adjacent tissue, respectively[54]. The interstitial fluid of mouse melanoma was also found to be depleted of glucose, again on a scale of a 10-fold reduction compared to blood and healthy splenic tissue[55]. As tumors grow, the cores may become increasingly hypoxic, and the cancer cells may become increasingly dependent on anaerobic metabolism (i.e. glycolysis). As a result, tumors that have progressed for longer host lower concentrations of glucose compared to newer tumors that are smaller in size[56].

Genetic mutations result in cancer cells that are intrinsically wired to engage in elevated rates of glucose metabolism, regardless of negative environmental feedback. Additionally, tumors develop disorganized tissue architectures, resulting in poor perfusion and poor oxygen delivery, and as a result, glycolysis is further reinforced. Voracious consumption of glucose by the tumor and inefficient resupply of glucose by perfusion results in a net depletion of glucose from the tumor environment, which can impact all cells present in the tumor, including those from the immune system.

CHAPTER 2

T CELL METABOLISM IN HEALTH AND CANCER

2a. Cytotoxic T cells Control Tumors

Mutations that potentiate the transformation of a cell from normal to malignant occur at a high frequency, arising from hereditary, environmental, and replicative sources[57]. As a result, cancerous cells develop within our bodies at a remarkably high rate[58,59], but the incidence of full-blown tumors is much lower due to the ability of our immune system to eliminate cells once they have transformed. This process, known as immunosurveillance, was controversial when it was first suggested over a century ago[60], but experimental evidence over the last several decades has confirmed the important role that lymphocytes play in controlling tumor outgrowth[61–66]. The definitive work demonstrating immunosurveillance was performed using mice hosting a defective recombination activation gene 1 (RAG-1) or RAG-2, which completely lack lymphocytes (including natural killer cells, T and B cells)[67]. RAG-1 and RAG-2 knockout mice developed cancer more rapidly and with greater frequency than controls[68]. Immunosurveillance of human tissue is supported by a preponderance of evidence showing the association between immune activity and tumor progression[69,70]. Indeed, clinical data has demonstrated tumor-infiltrating T-cell density as an independent prognostic marker in a variety of cancers including oral squamous cell, colorectal, and ovarian carcinomas[71–74].

Immune mediated suppression of tumors is dependent on the capacity of lymphocytes to distinguish healthy cells from those that have acquired mutated or foreign proteins. These non-self proteins may arise from various mechanisms, including genomic mutation, transcriptomic variation, post-translational modification, and viral open reading frames[75,76] and are referred to as neoantigens. T cells contain receptors (TCRs) that can recognize neoantigens from proteins that have been phagocytosed and processed by antigen presenting cells (APCs), which are then presented on the cell surface in the context of major histocompatibility complex (MHC) proteins. The recognition of neoantigen peptide:MHC complexes is the basis for T cells to distinguish between healthy and cancerous cells. Recently, a great deal of effort has been put forth to identify

cancer neoantigens, with the goal of equipping or identifying immune cells with the appropriate receptors for these antigens, expanding them ex vivo, and infusing them into patients as a form of cell mediated therapy. This is the basis for the rapidly growing field of TCR- and chimeric antigen receptor (CAR)-T cell therapy. Although significant effort has been put forth to describe antigens that are unique to cancer cells and shared among many tumors, few if any have been identified. Instead, alternative approaches have been employed wherein immune cells are equipped with receptors that recognize normal, self-antigens, but are differentially expressed in cancer tissue or on a cell population that is deemed non-essential. For example, the most prevalent form of CAR-T therapy clinically employed today targets a B cell antigen abundantly expressed on both B cell lymphomas and healthy B cells. This approach ablates the entire mature B cell population (cancerous or healthy) but is regarded as a tolerable side effect compared to the cancer itself.

Once a T cell has identified the appropriate target, it may initiate cytotoxic activity, the defining function of cytotoxic CD8+ T cells. This occurs only after the TCR or CAR has bound to the target antigen, which triggers the formation of an immunological synapse. Immunological synapses are structures formed between T cells and their targets that mediate the transfer of cytotoxic material stored in lysosomal compartments known as cytolytic granules. Within cytolytic granules are perforin-1 and calreticulin, pore forming proteins that create a physical opening in the target cell plasma membrane. Once the pore has formed, vesicles within the T cell are delivered to the cell surface, which then release pro-apoptotic proteases (granzymes) that passively diffuse into the target cell. Granzyme proteases induce programmed cell death (apoptosis) primarily by cleaving caspase-3, which plays a dominant role in initiating the apoptotic cascade that ultimately results in cell death. The delivery of perforin and granzymes to target cells to induce the apoptotic cascade is the primary means by which immunosurveilling lymphocytes kill transformed cancer cells.

2b. Activated T cells Undergo Metabolic Rewiring to Support Function

Prior to ligation of the TCR, naïve T cells are quiescent - a state of dormancy with low basal metabolic rates and infrequent cell divisions. As naïve T cells circulate throughout the body to secondary lymphoid tissues and surveil for antigens, they must engage in cytoskeletal rearrangements that are energetically expensive but require only basal rates of biosynthesis. Resting T cells therefore have metabolic profiles that on balance favor energy production over biosynthesis. Therefore, the oxidation of fatty acids and glutamine (which powers mitochondrial respiration) generate sufficient energy for naïve T cells as they surveil the body[77].

Once a T cell has been activated, it must grow, proliferate, and exhibit effector function, including the production and secretion of effector molecules such as cytokines and granzymes. These are all resource intensive processes that dramatically increase the metabolic requirements of a stimulated T cell. Just like the rapidly proliferating and cancer cells described in the previous chapter, T cells strongly upregulate the use of aerobic glycolysis to support their metabolically demanding activities. Signaling through the TCR complex potentiates the glycolytic transition through both transcriptional and post-translational mechanisms. TCR ligation rapidly induces the expression of the transcription factor c-Myc, a cell cycle and metabolism master regulator that induces expression of *all* of the genes involved in the core glycolytic pathway, including strong inductions of Glut1, Hk2, and Ldha[78,79]. At the post-translational level, the intracellular domain of the TCR complex recruits pyruvate dehydrogenase kinase (PDHK), where it is then activated through phosphorylation, and in turn phosphorylates PDH. Phosphorylation of PDH inhibits the conversion of pyruvate into acetyl-CoA, in effect directing pyruvate away from oxidation in the mitochondria and instead towards reduction into lactate, with a concomitant oxidation of NADH[80]. The net result of the shift in pyruvates fate is the production of oxidized NAD (NAD+), which can be recycled into upstream reactions involved in glucose oxidation, enabling glycolysis to continue to turnover at a rapid rate.

Secondary signals, like ligation of CD28 or 41BB, are required for complete T cell activation. In the absence of these signals, T cells become anergic, a nutrient deficient and hyporesponsive state[81]. Signaling through these coreceptors allows T cells to increase their glycolytic rate to a level that can sufficiently support the robust proliferative burst that T cells experience following activation[82]. CD28 costimulation increases Glut1 surface expression via PI3K/AKT signaling, allowing for increased glucose uptake, glycolysis, and lactate production[83]. 41BB costimulation acts through the LKB1-AMPK-ACC signaling pathway to increase Glut1 expression, also increasing the levels of glucose uptake over TCR ligation alone[84]. CD28 and 41BB costimulation need not occur simultaneously, but in the absence of either of these secondary signals, T cells will not sufficiently rewire the metabolic circuits that are required to support the energetic and anabolic demands of fully activated T cells[82].

Beyond TCR and coreceptor stimulation, T cells receive environmental inputs from soluble factors, including the cytokine IL-2. IL-2 can be both generated and sensed by CD8+ T cells, allowing it to act in an autocrine fashion. IL-2 ligation activates several signaling pathways, including PI3K/AKT and ERK/MAP, resulting in strong induction of cell cycle activity[85,86]. IL-2 activation also promotes MYC and mTORC1 signaling to be sustained in the absence of TCR ligation, allowing T cells to maintain elevated rates of metabolism and proliferation during transit between the antigen presenting cell and the target for killing[87]. HIF1a activity is also induced downstream of IL-2/mTORC1 signaling and is the primary mediator of the ability for mTORC1 to induce a glycolytic program in T cells[88].

The myriad of signal transduction events that T cells undergo during activation converge to generate a phenotype significantly more capable of robustly carrying out and engaging glycolysis. As previously discussed, aerobic glycolysis is an important means of generating the anabolic precursors needed during times of intense cell growth and proliferation, which is an important duty of freshly activated T cells. But glycolysis also plays an important role in modulating

T cell function beyond providing building blocks for macromolecular synthesis. As the rates of glucose uptake and catabolism increase within the cell, glycolytic metabolites including glyceraldehyde 3-phosphate (GAP) begin to accumulate and occupy the active site of the enzyme glyceraldehyde 3-phosphate dehydrogenase (GADPH). This occupancy of GAPDH by its substrate prevents it from participating in alternative functions, including preventing the translation of mRNAs containing AU rich elements in their 3' UTRs. Interferon-γ (IFNg) is one such mRNA and is transcribed at significantly elevated levels post activation. As glycolysis is ramped up and GAP accumulates, GAPDH spends more time catalyzing the conversion of GAP and less time preventing the translation of AU rich mRNAs, resulting in increased translation of IFNg[89]. IFNg expression is also enhanced through epigenetic modifications that result from increased rates of aerobic glycolysis. As LDHA activity increases during aerobic glycolysis, more citrate is exported from the mitochondria, resulting in an accumulation of acetyl-COA and acetyl histone modifications that increase IFNg transcription[90].

Overall, T cell metabolism is dynamic and extremely sensitive to environmental cues. Upon activation, T cells robustly engage in glycolysis and use the pathway to support a burst in cell cycling, as well as to enforce effector functions such as cytokine production and cytotoxicity.

2c. Tumor Environment Negatively Impacts T Cell Metabolism and Function

While the immune system plays an essential role in elimination of newly formed tumor cells, immunoediting can impose a selective pressure that results in tumor cells capable of evading immune-mediated destruction. This process, referred to as “escape”, is mediated by a variety of mechanisms that serve to limit or disrupt immune function[91]. Among these inhibitory processes, are those that exert influence on the immune system through metabolic means. One such mechanism is through the upregulated expression of LDHA seen in transformed cancer cells undergoing elevated rates of aerobic glycolysis. As LDHA activity increases, large quantities of lactic acid are excreted from the rapidly growing cells, saturating the tumor environment with protons and lactate that can negatively impact immune surveillance[92,93]. Some tumors harbor mutations that activate the enzyme indoleamine 2,3-dioxygenase (IDO), resulting in increased conversion of tryptophan into kynurenine, a metabolite detrimental to T cell proliferation and function[94]. In addition to these metabolic derangements, several processes lead to a dearth of glucose in the tumor environment (as discussed in Chapter 1).

The absence of glucose from tumor tissue poses a serious challenge for tumor infiltrating T cells, as aerobic glycolysis is strongly engaged during T cell activation and is relied upon to support effector function. The negative impact of glucose withdrawal has been extensively demonstrated in blasting, activated T cells. T cell *survival* is dependent on sufficient glycolytic flux to prevent the Bcl-2 family of proapoptotic factors from becoming activated and inducing apoptosis[95]. T cell *proliferation* is extremely sensitive to the availability of glucose in the environment, as demonstrated through studies employing glucose titration and pharmacologic or genetic inhibition of glycolysis[21,79,82,96]. T cell *cytokine output* is also profoundly sensitive to glucose withdrawal, with IFNg transcription and translation showing a high dependency on glucose and glycolytic turnover[95,97–99]. Glucose deprivation also curtails *cytotoxicity* and killing capacity of CD8+ T cells, through reduced production of effector molecules including granzyme

A, B, and C[98,100,101]. Importantly, many of the functions that are lost upon glucose withdrawal, including cytokine and effector molecule production, can be restored upon reintroduction of glucose into the environment[99,102].

As tumor infiltrating T cells penetrate tumor tissue, they find themselves surrounded by cancer cells that are hard-wired to voraciously consume glucose. As both cancer cells and T cells maintain high glycolytic flux to sustain their metabolically demanding cellular activities, and as glucose levels plummet in the tumor environment, competition for the remaining supply of glucose commences. The concept of metabolic competition for a limited glucose supply was demonstrated by Chang et al. in a study showing that the glycolytic profile of a tumor is capable of influencing the glycolytic profile of the tumor infiltrating T cells, via glucose depletion in the tumor environment[103]. In experiments where the glycolytic output of tumors was manipulated, the tumors with the highest rates of glycolysis hosted T cells with the inverse metabolic profiles – that is, lower rates of glycolysis and a higher dependence on oxidative respiration. The inability of T cells to fully satiate glycolytic demand was shown to negatively impact the production of IFNg and ultimately led to tumor progression. In humans, clinical evidence suggests that tumors with higher rates of glycolysis host less and/or dysfunctional T cells. In a cohort of 47 patients with melanoma, those with lower levels of expression of glycolysis related genes had an increased probability of progression free survival times[104]. In head and squamous and renal cell carcinomas, increased levels of tumor glycolysis correlated with decreased CD8+ T cell infiltration[105,106].

Adoptive cell transfer has revolutionized the treatment of liquid cancers through redirection of T cell targeting, but solid tumors still generate environments that are barren of the critical fuel source glucose, detracting from therapeutic efficacy[103,107]. One strategy to increase the environmental availability of glucose for T cells as they penetrate tumors is to target tumor

glycolysis with pharmacologic inhibition, but this approach has the undesired consequence of nonspecifically inhibiting glycolysis in the CD8+ T cells that are meant to control the tumors[104]. Instead, we propose an alternative strategy wherein tumor infiltrating T cells are metabolically enhanced. This can be achieved by providing a glucose source that ***exclusively*** fuels T cells and is incapable of being metabolized by cancer cells. This would allow tumor-infiltrating T cells to engage aerobic glycolysis at higher levels and enhance their effector function, regardless of the glucose consumption rates of the surrounding cells, therefore bypassing any competition for this limited resource. This approach depends on identifying a glucose containing compound that is inert to human metabolism. Cellobiose, a glucose disaccharide, is a candidate with many desirable properties.

CHAPTER 3

DEVELOPING A THERAPY: CELLOBIOSE AS A FUEL SOURCE

3a. Cellobiose in the Environment and our Bodies

Cellulose is the most abundant organic polymer on Earth[108]. It is the primary skeletal component of plant cell walls and is composed of repeating units of D-glucose. Each glucose is linked to the next via a β (1→ 4) bond, resulting in the disaccharide cellobiose, and may extend for hundreds to thousands of additional units. Cellobiose, which is harvested industrially through the saccharification of cellulose, is extremely cheap to obtain due to the prevalence of cellulose in the environment[109] (in 2023, one kilogram of a molecular biology grade reagent can be obtained for roughly one thousand dollars).

Cellobiose is extremely stable in the environment and requires acid or enzymatic treatment for hydrolysis[110,111]. Many different microbial organisms, including bacteria and fungi, have evolved the capacity to use cellobiose as a fuel source by expressing enzymes that hydrolyze the β (1→ 4) bond joining the two glucose molecules in cellobiose, yielding free glucose that can be metabolized via the standard glycolytic pathway. Some microbes secrete these hydrolases into the extracellular space, where cellobiose hydrolysis occurs, and then rely on glucose transporters to acquire the glucose product[112]. Other microbes have evolved transporters that translocate cellobiose into the intracellular space where it is then hydrolyzed by the glycosidases[113].

Surprisingly, animals have not evolved the appropriate proteins to use the abundance of cellobiose in the environment as a fuel source, perhaps due to the complex bonds that can be found in lignocellulosic material. Some animals, like cows and other ruminants, have developed chambered stomachs that host dense microbial colonies that can access the nutrient potential locked away in the β (1→ 4) cellobiose bond[114]. For others, including mice and humans, cellobiose passes through the small intestine undigested before reaching the colon, where it is partially

digested by enteric microbes[115]. The undigested remainder acts as fiber and a stool bulking agent[116,117].

Despite the indigestibility of cellobiose and the unnatural presence within mammalian systems, several studies have studied the introduction of cellobiose directly into the blood of mammals for various applications. In separate studies that measured the retention of cellobiose after intravenous injection in human and pig, greater than 95% of cellobiose was recovered in the urine, confirming that mammalian systems do not harbor the necessary enzymes to metabolize cellobiose[118,119]. In one of these studies, cellobiose was continuously infused for 120 hours, after which kidney histological analysis demonstrated no pathological processes occurring in the tubules or glomeruli[118]. Likewise, other studies implementing intravenous cellobiose administration reported no toxic side effects, including those conduced in humans[119,120].

3b. Engineering Cellobiose Metabolism

The breakdown of cellulosic content has generated interest in industrial settings, primarily in the context of biofuel production[121]. To that end, many of the genes and proteins that are involved in cellobiose transport and hydrolysis have been identified and characterized[110]. The heterologous expression of many of these cellobiose catabolism genes has been well studied, primarily in the model organism *Saccharomyces cerevisiae*[122–127]. From these studies, two genes from the fungus *Neurospora crassa* have been identified that enable *S. cerevisiae* to efficiently carry out cellobiose metabolism.

Cellodextrin transport-1 (cdt-1) is a 63 kD protein that localizes the plasma membrane and enables co-transport of cellobiose and a proton down the concentration gradient, from the extracellular space into the cytosol of the cell[122]. The proton must then be pumped out of the cell, requiring one unit of ATP in the process. *Neurospora* also expresses the cdt-1 isoform cellodextrin transport-2 (cdt-2), which does not require a proton for co-transport and is thus more energetically efficient[128]. The heterologous expression of cdt-2 results in less robust growth using cellobiose, indicating that the transporter is not as efficient at transporting cellobiose[125]. Efforts have been made to engineer cdt-1 and cdt-2 to enhance cellobiose transport capacity, but none have gained widespread traction[127,129,130]. Alternatives to *Neurospora* cellobiose transporters have been identified, although their functional capacity has generally not been demonstrated to be superior to that of cdt-1[131–133].

Glycosylhydrolase family 1-1 (GH1-1) is a 54 kD protein that localizes to the cytosol and catalyzes the hydrolysis of the β (1→ 4) cellobiose bond, yielding free glucose[122]. GH1-1 has served as the workhorse of engineered cellobiose catabolism, as it has efficiently carried out cellobiose hydrolysis in a variety of systems across different research laboratories. Alternative methods to free glucose from cellobiose have been identified, including the use of phosphorolytic

enzymes, which can catalyze the conversion of cellobiose and inorganic phosphate into one molecule of glucose and one molecule of glucose-6-phosphate. By directly producing one molecule of glucose-6-phosphate from cellobiose without the use of ATP, cellobiose phosphorylases present an energetically favorable means of initiating glycolysis, due to bypassing the phosphorylation of glucose with HK2 and ATP[129]. While phosphorolytic enzymes have successfully been expressed via plasmid delivery systems in *S. cerevisiae*, their utilization in viral gene delivery systems is hampered by their large size. The most efficient cellobiose phosphorylase studied to date, SdCBP, is ~800 amino acids long (~2.4 kilobases), which, depending on the accessory genetic cargo, may generate large viruses that are inefficiently packaged.

There are several important considerations when designing a virus that will deliver genetic cargo and enable heterologous expression of a transgene. Amongst the most impactful considerations when implementing an expression system for cellobiose catabolism is the expression levels of the transgenes[127,134–136], with higher levels of expression being demonstrated to be a limiting factor in the rates of cellobiose catabolism. To achieve efficient protein translation in mammalian systems, the amino acid codon frequency encoded in the transgenic transcripts must resemble the relative abundance of tRNAs in mammalian cells. The conversion of amino acid sequences into transcripts that are efficiently translated is known as codon optimization, and importantly, the algorithms that generate optimized codon sequences are not deterministic[137]. Therefore, it is important when testing codon optimized genetic variants, to test multiple variants and empirically determine which variants result in the highest levels of expression. A second consideration is the promoter that is used to drive expression. Different promoters drive expression with different efficiencies, and the efficiency is largely dependent on cell type. Finally, for genes of interest for which there no antibodies have been developed, it is important to add a peptide epitope tag for immunostaining analysis.

By inserting codon optimized, transgenic sequences into viral vectors that are optimized for robust expression and transduction of target cells, cellobiose catabolism may be enabled through the co-expression of cdt-1 and gh1-1.

CHAPTER 4

ENHANCING TUMOR-INFILTRATING T CELLS WITH CELLOBIOSE

Enhancing tumor-infiltrating T cells with an exclusive fuel source

Matthew L. Miller[1,2], Rina Nagarajan[3], Timothy J. Thauland[3], Manish J. Butte[1,2,3,4,*]

1. *Molecular Biology Institute, UCLA; Los Angeles, CA, USA.*
2. *Department of Microbiology, Immunology, and Molecular Genetics, UCLA; Los Angeles, CA, USA.*
3. *Division of Immunology, Allergy, and Rheumatology; Department of Pediatrics, UCLA; Los Angeles, CA, USA.*
4. *Department of Human Genetics, UCLA; Los Angeles, CA, USA.*

** Corresponding author*

Correspondence:

Manish J. Butte, MD PhD
David Geffen School of Medicine at UCLA
650 Charels E. Young Drive South, CHS 46-100
Los Angeles, California 90095
Phone: (650) 384-9149
Email: mbutte@mednet.ucla.edu

SUMMARY

Solid tumors harbor immunosuppressive microenvironments that inhibit tumor-infiltrating lymphocytes (TILs) through the voracious consumption of glucose. We sought to restore TIL function by providing them with an exclusive fuel source. The glucose disaccharide cellobiose, which is a building block of cellulose, contains a β-1,4-glycosidic bond that cannot be hydrolyzed by animals (or their tumors), but fungal and bacterial organisms have evolved enzymes to catabolize cellobiose and use the resulting glucose. By equipping T cells with two proteins that enable import and hydrolysis of cellobiose, we demonstrate that supplementation of cellobiose during glucose withdrawal restores T cell cytokine production and cellular proliferation. Murine tumor growth is suppressed, and survival is prolonged. Offering exclusive access to a natural disaccharide is a new tool that augments cancer immunotherapies. Beyond cancer, this approach could be used to answer questions about the regulation of glucose metabolism across many cell types, biological processes, and diseases.

INTRODUCTION

Glucose is a critical fuel for cellular bioenergetics and a major source of biosynthetic precursors for anabolic pathways. Upon antigen stimulation, CD8+ T cells extensively rewire their metabolism and robustly engage aerobic glycolysis to support the various functions required of cytotoxic T cells, including survival, proliferation, cytokine production, and cytotoxicity. Abnormally low glucose concentrations are found in the tumor microenvironment (TME) of solid tumors due to the voracious nature of tumor metabolism, leading to a competition for glucose that contributes to cancer progression[89,90,138–143] due to stunted T-cell effector functions[55,80,98,99]. We hypothesized that TILs provisioned with an *exclusive* source of glucose that was inaccessible to cancer cells would be invigorated, allowing them to fulfill their role in clearing tumors more effectively.

Cellobiose, a glucose disaccharide that comprises cellulose and is found abundantly in plant matter, has great potential to serve as a carbon and energy source but remains inert to catabolic processes in animal cells for two primary reasons. First, metazoan sugar transport is restricted to monosaccharides. Second, the β-1,4-glycosidic bond that joins glucose molecules in cellobiose cannot be efficiently hydrolyzed by metazoan glycoside hydrolases[115,118]. The transport and hydrolyzation of cellobiose, on the other hand, can be efficiently carried out in cellulolytic microbes such as fungi and bacteria[122,144,145]. Thus, cellobiose could offer an exclusive source of glucose for engineered T cells, as it is inaccessible to tumors.

Here, we report that the heterologous expression of a cellobiose transporter and a β-glucosidase from the mold *Nuerospora crassa* in primary T cells endows them with the ability to robustly catabolize cellobiose, which rescues T cells from glucose deprivation. We demonstrate that tumor cells lack the ability to use cellobiose, allowing this nutrient to exclusively support the metabolism of T cells. Finally, we show that enabling engineered T cells to overcome the glucose restriction of the tumor microenvironment allows for an increased capacity to clear tumors.

RESULTS

Heterologous and Functional Expression of Cellobiose Catabolism Proteins in Primary T cells

To impart the ability to catabolize cellobiose as a fuel source for glycolysis, only two proteins are needed: 1) a transporter of cellobiose from the extracellular to intracellular space; and 2) a β-glucosidase that can efficiently hydrolyze the β-1,4 bond that joins the glucose molecules in cellobiose. We chose to work with a pair of previously characterized proteins from *Neurospora crassa*, namely, the cellobiose transporter CDT-1 and the cellobiose glucosidase GH1-1 **(Fig. 1a)**, which were reported to enable cellobiose catabolism through heterologous expression into yeast[122].

We optimized the codon sequence of each gene for murine expression **(Fig. S1)** and cloned them into mouse stem cell viral vectors **(Fig. 1b)**. Each transgene was appended with a hemagglutinin (HA) tag and coupled to a discrete fluorescent protein via a 2A peptide sequence. Staining of transduced, primary CD8+ T cells for the HA tag revealed robust expression of both genes, which was demonstrated to be coupled to their fluorescent reporters **(Fig. 1c)**. To confirm the subcellular localization of each protein, we immunostained T cells and performed confocal microscopy. CDT-1 localizes to the periphery of the T cell, which is consistent with its function as a transporter. In contrast, the distribution of GH1-1 is more diffuse, indicative of a cytosolic localization and consistent with the localization of other enzymes involved in the glycolytic pathway[146] **(Fig. 1d)**.

We next sought to confirm the functionality of each transgenic protein. To test the capacity of CDT-1 to transport cellobiose, we incubated transduced T cells with cellobiose, extracted intracellular metabolites, and performed liquid chromatography-mass spectrometry (LC-MS). We found that cellobiose accumulated in the intracellular metabolite pool at a higher rate in T cells

expressing CDT-1 compared to control cells **(Fig. 1e)**. To evaluate the functionality of GH1-1 as a cellobiose glucosidase, we transduced T cells with GH1-1, generated cellular lysates, incubated with cellobiose, and quantified the resultant glucose yield. We found that GH1-1 expression significantly increased the glucose concentration over time **(Fig. 1f)**. Taken together, we have developed a system wherein primary T cells co-transduced with the genes CDT-1 and GH1-1 (referred to as CG-T cells) are endowed with the necessary machinery to utilize extracellular cellobiose as a source of intracellular glucose.

Transgenic T cells Robustly Catabolize Cellobiose to Fuel Glycolysis

To test if CG-T cells are capable of catabolizing cellobiose, we incubated control and CG-T cells with copious, isotopically labelled U-$^{13}C_{12}$ cellobiose in the presence of a low concentration of unlabeled glucose **(Fig. 2a)**. We observed extensive carbon labeling in key metabolites of the glycolytic, pentose phosphate, and tricarboxylic (TCA) pathways in CG-T cells **(Fig. 2b)**, with cellobiose contributing nearly 100% of the carbons present in glycolytic metabolites such as fructose 1,6-bisphosphate, 3-phosphoglyceric acid, and phosphoenolpyruvate. In stark contrast, control cells showed negligible labeling of intracellular metabolites, an expected result that confirms our conventional understanding that mammalian cells lack the capacity to metabolize cellobiose.

To determine whether cellobiose carbons are fluxing through the standard glycolytic pathway, we incubated the transduced T cells with isotopically labeled glucose (U-$^{13}C_6$) and compared glucose metabolite labeling to cellobiose metabolite labeling. This comparison in CG-T cells revealed a striking similarity in the distribution profile of catabolized cellobiose carbons to glucose carbons **(Fig. 2b)**, demonstrating that cellobiose carbons are flowing through the standard metabolic pathways. When comparing glucose catabolism in CG- versus control T cells, the distribution profiles of glucose carbons again look nearly identical, demonstrating that

transgenic expression of CDT-1 and GH1-1 did not result in any changes in the fate of catabolized glucose carbons. These results confirm that our approach allows cellobiose catabolism to replace the role of glucose in feeding metabolic pathways.

Glucose deprivation in T cells leads to profound metabolic perturbations, with reductions in the amounts of metabolites from the glycolytic, glycosylation, pentose phosphate, and tricarboxylic acid (TCA) pathways, and the accumulation of low-energy and oxidative intermediates including NAD+, AMP, and oxidized glutathione (GSSG) **(Fig. S2)**. To assess whether CG-T cells can use cellobiose to normalize metabolite abundances during glucose withdrawal, we compared the abundance of metabolites during incubation with cellobiose to the abundances during incubation with glucose. CG-T cells incubated with cellobiose showed rescue of core glycolytic metabolites (glucose, F16BP, and acetyl-CoA), intermediates derived from glycolysis that contribute to protein glycosylation (UDP-glucose, GlcNAc-6P, and UDP-GlcNAc), and precursors of purine and pyrimidine synthesis (ribose-5-phosphate, phosphoribosyl pyrophosphate, and inosine monophosphate) **(Fig. 2c)**. Furthermore, incubation with cellobiose normalized levels of metabolites central to mitochondrial function, with increased amounts of TCA substrates (acetyl-CoA, citrate, aconitate, and α-ketoglutarate) and the accumulation of a reduced chemical environment (NADH, ATP, and GSH) **(Fig. 2c)**. These results demonstrate that in CG-T cells, cellobiose is catabolized into glucose, which then replenishes several of the major metabolic pathways that are depleted during glucose deprivation.

To compare the glycolytic output of CG-T cells using cellobiose versus glucose as fuel sources, we conducted sugar stress tests using the Seahorse platform, wherein the starting condition entailed complete glucose deprivation and then the first injection was either glucose or cellobiose. CG-T cells exposed to cellobiose led to robust engagement of glycolysis, demonstrated by a ~2-fold increase in extracellular acidification rate (ECAR). Control T cells did not change ECAR when exposed to cellobiose. As expected, glucose exposure equivalently

increased ECAR in both control T cells and CG-T cells **(Fig. 2d)**, again demonstrating that the transgenes do not alter the capacity to engage glycolysis. These results confirm the ability to use cellobiose as a fuel source. The discrepancy between ECAR increase seen when CG-T cells were exposed to glucose versus cellobiose may be impacted by the mechanism of CDT-1 transport, namely that a proton is transported into the cell along with cellobiose **(Fig. 1a)**. As catabolism of cellobiose generates protons that are excreted into the media, CDT-1 transport of cellobiose removes protons from the media, ultimately diminishing the net readout of extracellular acidification. Together, these findings demonstrate that the profound metabolic disturbances experienced by T cells upon glucose withdrawal can be ameliorated by cellobiose through the expression of CDT-1 and GH1-1.

Effector Function of Transgenic T cells is Fueled by Cellobiose During Glucose Withdrawal

Activated T cells are critically dependent on glucose for optimal anti-tumor activity, as reductions in glucose negatively impact survival, proliferation, and cytokine production. To validate whether cellobiose could rescue these functions in transgenic T cells during glucose deprivation, we next performed a series of in vitro tests.

To assess whether cellobiose could enhance T-cell survival during glucose withdrawal, we incubated T cells ± glucose ± cellobiose for 48 h. Under light microscopy, control T cells incubated with glucose appeared large, polarized, and healthy. In contrast, glucose-deprived cells adopted the distinct morphological characteristics of dead and dying cells – that is they appeared small, shriveled, and/or blebby **(Fig. 3a)**. The presence of cellobiose had no discernible effect on morphology in control cells. CG-T cells incubated with and without glucose appeared the same as their control counterparts but the inclusion of cellobiose during glucose withdrawal rescued vitality and cellular morphology akin to cells incubated with glucose. Thus, cellobiose can extend

survival in CG-T cells during glucose withdrawal. We further assessed the same cell populations and their morphological characteristics by flow cytometry. When incubated with glucose, a high fraction of the control cells was large and had low granularity (FSC^{hi}, SSC^{lo}) **(Fig. 3b)**. The absence of glucose shifted the cell population towards a FSC^{lo}, SSC^{hi} phenotype, commonly interpreted as dead and dying compared to their large, low granularity counterparts. Again, the presence of cellobiose made little difference for control cells. In contrast, CG-T cells incubated with cellobiose during glucose withdrawal shared the morphology of cells incubated with glucose, demonstrating that transgenic CG-T cells sustained their viability when using cellobiose as a metabolic substrate.

To determine whether cellobiose could not only extend survival but also support the more resource and energy intensive process of cell division, transduced T cells were labeled with the cell proliferation dye CellTrace Violet (CTV). After CTV staining, the cells were incubated for 48 h in high to low concentrations of glucose and cellobiose was added or omitted at each concentration. We assessed proliferation by the dilution of CTV as measured by flow cytometry. As expected, reducing glucose concentration resulted in less dilution of the CTV signal (i.e., less cell proliferation) in control and CG-T cells, but the inclusion of cellobiose allowed only CG-T cells to proliferate robustly, even at the lowest glucose condition tested that otherwise eliminates proliferation **(Fig. 3c)**. The proliferation of CG-T cells with cellobiose was comparable to their division seen at the highest concentration of glucose **(Fig. 3d)**. Thus, cellobiose robustly supports T cell proliferation in low glucose contexts.

To measure the extent to which cellobiose can fuel cytokine production during glucose withdrawal, CG-T cells were incubated in high or low glucose ± cellobiose overnight and then restimulated with PMA/ionomycin. Glucose withdrawal profoundly reduced the production of IFN-γ and TNF, an effect seen in the percent of cytokine positive cells and the concentration of the cytokines in the supernatant **(Fig. 3e,f; Fig. S3)**. During glucose withdrawal, CG-T cells that were

incubated with cellobiose restored IFN-γ and TNF production. Thus, cellobiose fuels cytokine production in low glucose contexts.

Taken together, we show that two major effector functions of T cells—proliferation and cytokine production—are rescued by cellobiose when glucose is critically low in T cells transduced with CDT-1 and GH1-1.

In vivo proof of concept

Many diverse metabolic perturbations develop in cancer cells, affecting the extent to which glucose is depleted from their TME. As a proof of concept for our approach, we sought a suitable model system of cancer in mice that conferred a low glucose microenvironment where cellobiose-metabolizing T cells could potentially thrive in the presence of cellobiose. We subcutaneously implanted into separate mice three different syngeneic cancer cell lines (EL4-OVA (lymphoma), B16-ND4 knockout (melanoma), and MC38-OVA (adenocarcinoma)). We compared the concentration of glucose in healthy tissues (spleen, peritoneum, and skin) to the concentration in these solid tumors by LC-MS. We found that EL4-OVA and B16-ND4 KO tumors consistently had significantly reduced concentrations of glucose compared to the healthy, adjacent tissues, and that EL4-OVA tumors were more depleted of glucose than all the healthy reference tissues **(Fig. S4a)**. All three types of tumors had samples with lower glucose concentrations than the healthy tissue, while MC38-OVA tumors were most heterogenous, with some tumors harboring low glucose levels and other tumors in the range of healthy tissue. Based on these results, we proceeded with the EL4-OVA model.

To determine the extent, if any, that the tumor cells themselves could benefit from the presence of cellobiose as a metabolic substrate, we incubated EL4-OVA cells in media lacking glucose but containing cellobiose and assessed the capacity to survive and divide. EL4-OVA cells were incapable of using cellobiose to facilitate proliferation **(Fig. S4b)**. Furthermore, live/dead

staining showed no survival advantage when cellobiose was provided in the absence of glucose **(Fig. S4c)**. These results confirm that cellobiose would exclusively be available to CG-T cells as a fuel source.

For cellobiose to be available as a fuel source for adoptively transferred T cells, it must be present in the blood in high concentrations. Providing cellobiose in food or water is not a viable means of increasing blood concentration of cellobiose, due to the low rates of para- and transcellular transport of cellobiose across the intestinal epithelium, in addition to the capacity for gut microbiota to metabolize cellobiose. Instead, we opted to deliver cellobiose through repeated intraperitoneal injections. To determine the appropriate dosing schedule of cellobiose, we monitored the concentration of cellobiose in the blood after i.p. injection by LC-MS. We found that after i.p. injection, the concentration of cellobiose went up sharply into the millimolar range and returned back down to baseline within 8 h **(Fig. S4d)**. Based on these results we decided to administer multiple cellobiose injections each day after the adoptive transfer of CG-T cells.

Finally, we tested the ability of CG-T cells fed with cellobiose to improve tumor clearance in a proof-of-concept experiment **(Fig. 4a)**. To provide for antigen-specific targeting of T cells to the tumor, we employed OT-I TCR transgenic T cells that recognize the ovalbumin antigen expressed by EL4-OVA tumors. We implanted EL4-OVA tumors subcutaneously on day 0. We activated OT-I T cells and transduced the CDT-1 and GH1-1 transgenes as above. T cells were injected i.v. on mice on day 10. Starting on the day of T cell adoptive transfer, we delivered either cellobiose or phosphate buffered saline (PBS, control) by twice daily i.p. injections in a blinded fashion. We measured the size of the tumors by calipers and assessed survival as determined by a tumor-size cutoff (see Methods) **(Fig. 4b)**. Survival was significantly improved in the mice receiving cellobiose injections (Cox regression, $p = 0.029$) **(Fig. 4c)**. The probability of survival at 30 days was 0.67 for mice treated with cellobiose and 0.25 for PBS. After the transfer of T cells, the median survival was 31 days for mice treated with cellobiose and 16 days for PBS. The hazard

ratio for survival was 2.95 (95% CI 1.1 to 7.8). At 4 weeks, progression-free survival (PFS) was five of 12 (42%) for mice receiving cellobiose and 8% for control-treated mice. Two of 12 (17%) mice receiving cellobiose showed a complete response whereas none of the PBS-treated mice survived long-term. These results show that tumor growth is more heavily suppressed and survival is prolonged in mice when treated with antigen-specific T cells capable of metabolizing cellobiose.

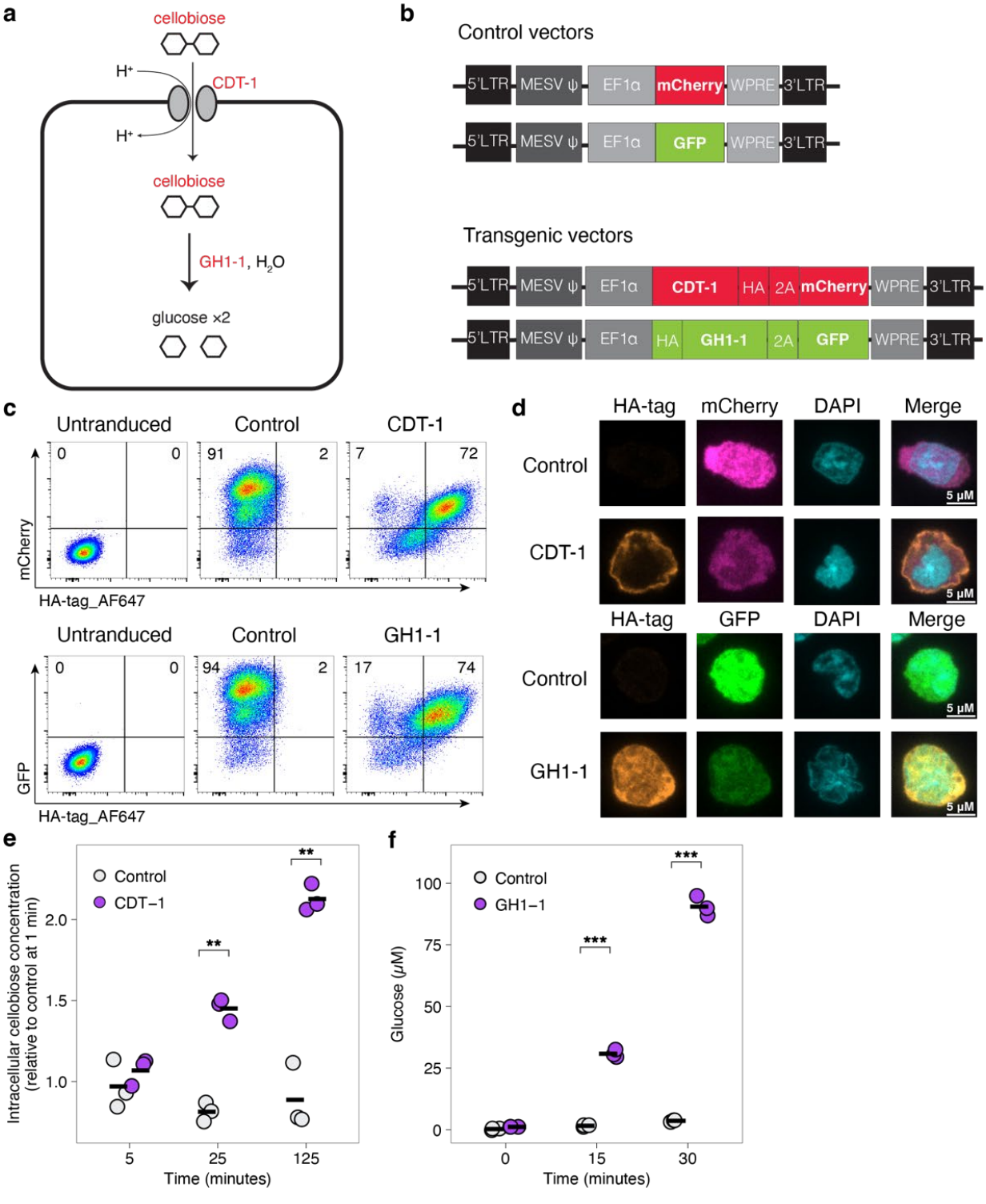
a
cellobiose
H+
CDT-1
H+
cellobiose
GH1-1, H2O
glucose ×2
b
Control vectors
5'LTR MESV ψ EF1α mCherry WPRE 3'LTR
5'LTR MESV ψ EF1α GFP WPRE 3'LTR
Transgenic vectors
5'LTR MESV ψ EF1α CDT-1 HA 2A mCherry WPRE 3'LTR
5'LTR MESV ψ EF1α HA GH1-1 2A GFP WPRE 3'LTR
c
Untranduced
Control
CDT-1
0
0
91
2
7
72
mCherry
HA-tag_AF647
Untranduced
Control
GH1-1
0
0
94
2
17
74
GFP
HA-tag_AF647
d
HA-tag
mCherry
DAPI
Merge
Control
CDT-1
5 μM
HA-tag
GFP
DAPI
Merge
Control
GH1-1
5 μM
e
Control
CDT−1
Intracellular cellobiose concentration (relative to control at 1 min)
2.0
1.5
1.0
**
**
5
25
125
Time (minutes)
f
Control
GH1−1
Glucose (μM)
100
75
50
25
0
***
***
0
15
30
Time (minutes)

Fig. 1. Heterologous expression of two proteins from fungi allow for cellobiose import and hydrolysis in T cells. **a)** Schematic of cellobiose transport through the proton symporter CDT-1, followed by hydrolysis by the cellobiose glucosidase GH1-1. Once glucose is liberated within the cell it may flow through the standard glycolytic pathway. **b)** Schematic of mouse stem viral vectors. Control vectors express fluorescent protein alone and transgenic vectors couple transgenic expression to fluorescent protein expression with a 2A peptide motif. Expression is driven by a constitutive EF1a promoter and enhanced with a woodchuck hepatitis virus post-transcriptional regulatory element (WPRE). **c)** Transgene and fluorescent protein expression analysis in transduced, primary, mouse T cells. **d)** Confocal microscopy images showing localization of CDT-1 (top) and GH1-1 (bottom), fluorescent proteins, and nuclei (DAPI) in transduced, primary, mouse T cells. **e)** CDT-1 transport assay. Control and CDT-1 transduced mouse T cells were incubated with 5 mM cellobiose before extracting intracellular metabolites for LC-MS quantification. **f)** GH1-1 hydrolysis assay. Control and GH1-1 transduced mouse T-cell lysates were incubated with 1 mM cellobiose before quantification of glucose with an Amplex Red glucose assay kit (Thermo). Horizontal lines indicate means. Statistical significance was assessed using an unpaired t-test in E and F (*$p < 0.05$; **$p < 0.01$; ***$p < 0.001$; NS > 0.05). Data shown in **e** and **f** are means of technical replicates (n=3) from one experiment and are representative of at least two independent experiments.

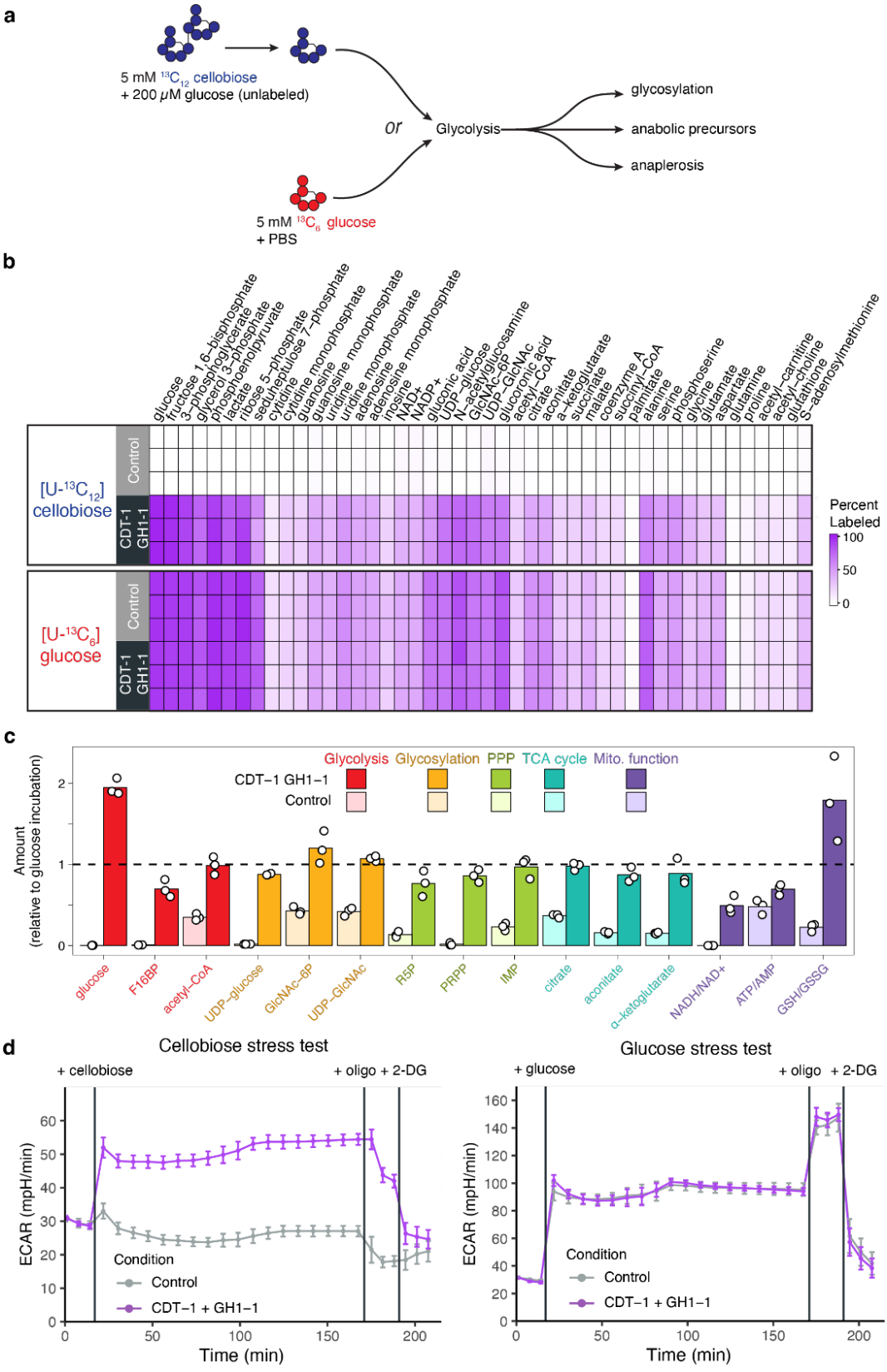
a
5 mM $^{13}C_{12}$ cellobiose
+ 200 μM glucose (unlabeled)
or
5 mM $^{13}C_6$ glucose
+ PBS
Glycolysis
glycosylation
anabolic precursors
anaplerosis
b
glucose
fructose 1,6–bisphosphate
3–phosphoglycerate
glycerol 3–phosphate
phosphoenolpyruvate
lactate
ribose 5–phosphate
sedoheptulose 7–phosphate
cytidine monophosphate
guanosine monophosphate
uridine
uridine monophosphate
adenosine monophosphate
inosine
NADH
NADP+
gluconic acid
UDP–glucose
N–acetylglucosamine
GlcNAc–6P
UDP–GlcNAc
glucuronic acid
acetyl–CoA
citrate
a–ketoglutarate
succinate
malate
coenzyme A
succinyl–CoA
palmitate
alanine
serine
phosphoserine
glycine
glutamate
aspartate
glutamine
proline
acetyl–carnitine
acetyl–choline
glutathione
S–adenosylmethionine
[U-$^{13}C_{12}$] cellobiose
[U-$^{13}C_6$] glucose
Control
CDT-1 GH1-1
Percent Labeled
100
50
0
c
Amount (relative to glucose incubation)
Glycolysis Glycosylation PPP TCA cycle Mito. function
CDT−1 GH1−1
Control
glucose
F16BP
acetyl–CoA
UDP–glucose
GlcNAc–6P
UDP–GlcNAc
R5P
PRPP
IMP
citrate
aconitate
α–ketoglutarate
NADH/NAD+
ATP/AMP
GSH/GSSG
d
Cellobiose stress test
+ cellobiose
+ oligo + 2-DG
ECAR (mpH/min)
Time (min)
Condition
Control
CDT−1 + GH1−1
Glucose stress test
+ glucose
+ oligo + 2-DG
ECAR (mpH/min)
Time (min)
Condition
Control
CDT−1 + GH1−1

Fig. 2. Transgenic T cells metabolize cellobiose and replenish metabolic pathways during glucose withdrawal. a) Schematic of isotopically labeled sugar experiment. Transduced T cells were incubated with either 5 mM universally 13C-labeled cellobiose and 200 μM unlabeled glucose or 5 mM universally 13C-labeled glucose for 16 h before intracellular metabolites were extracted for analysis by LC-MS. **b**) Heat map displaying the percent labeling of intracellular metabolites from transduced T cells incubated with isotopically labeled cellobiose or isotopically labeled glucose. **c**) Abundance of intracellular metabolites during cellobiose incubation relative to their abundance during glucose incubation. PPP, pentose phosphate pathway. **d**) Cellobiose and glucose stress tests using a XFe96 Seahorse Flux Analyzer. Transduced T cells had basal measurements taken before injection of cellobiose or glucose from the first port. Oligomycin A was injected from the second port and 2-deoxyglucose (2-DG) injected from the third port. ECAR, extracellular acidification rate. Error bars represent standard deviation of the mean, n=12. Data shown in b and c are from technical replicates (n=3) of one experiment and are representative of at least two independent experiments.

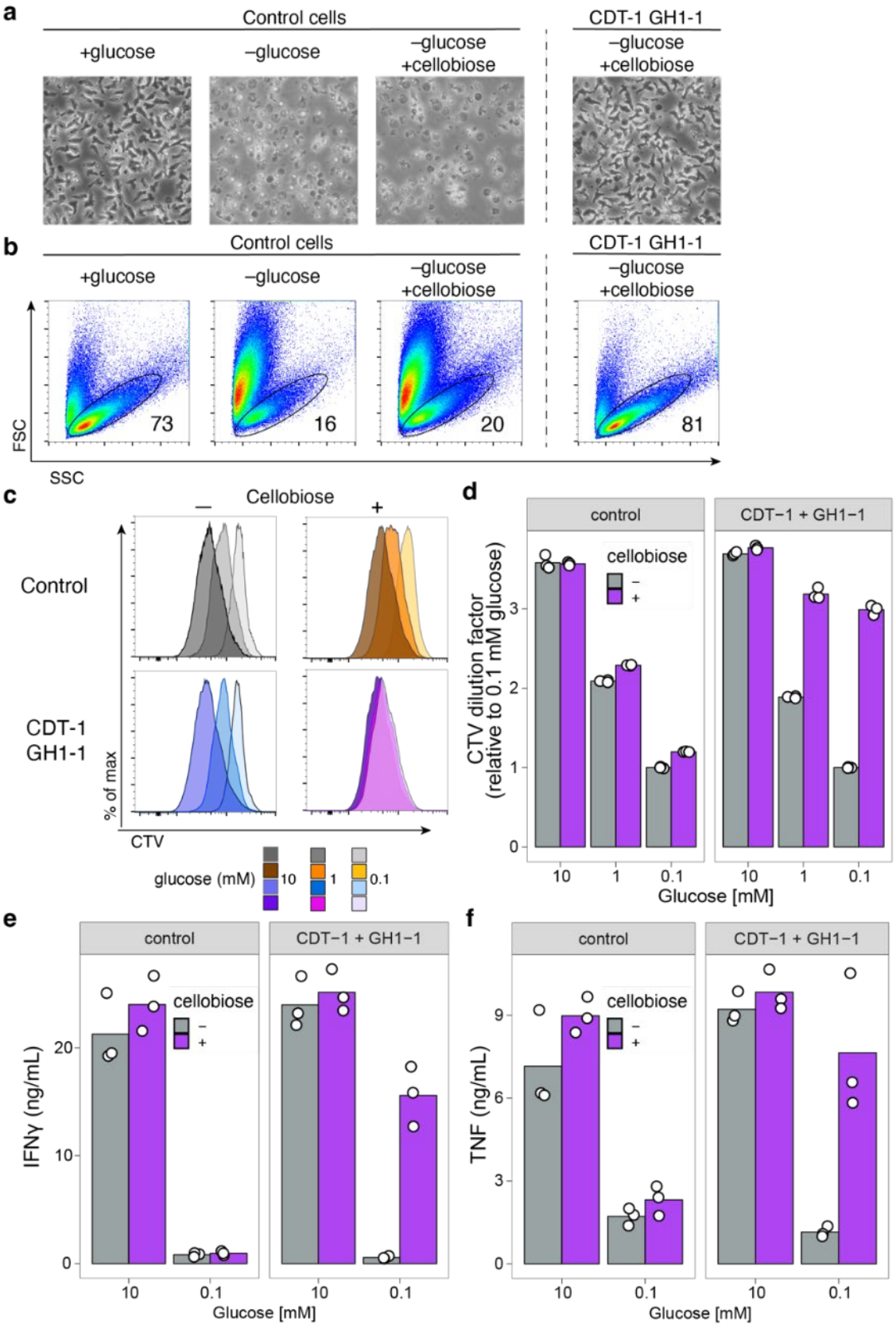
a
Control cells
+glucose
–glucose
–glucose
+cellobiose
CDT-1 GH1-1
–glucose
+cellobiose
b
Control cells
+glucose
–glucose
–glucose
+cellobiose
CDT-1 GH1-1
–glucose
+cellobiose
FSC
SSC
73
16
20
81
c
Cellobiose
—
+
Control
CDT-1
GH1-1
% of max
CTV
glucose (mM)
10
1
0.1
d
control
CDT−1 + GH1−1
cellobiose
–
+
CTV dilution factor
(relative to 0.1 mM glucose)
Glucose [mM]
e
control
CDT−1 + GH1−1
cellobiose
IFNγ (ng/mL)
Glucose [mM]
f
control
CDT−1 + GH1−1
cellobiose
TNF (ng/mL)
Glucose [mM]

Fig. 3. Cellobiose rescues effector functions in transgenic T cells. a) Light microscopy (4x objective) of transduced T cells after 48 hours in the indicated metabolic conditions. **b**) Flow cytometry was used to assess size (FSC) and granularity (SSC) of the same cell populations as imaged in (a). **c**) Transduced T cells were stained with CTV and immediately incubated in the indicated metabolic conditions for 48 hours, before measuring the extent of CTV signal dilution. Note that the using CTV to stain and analyze activated, cycling T cells does not produce discrete, halved signal peaks from each cell division (as is typically seen when this reagent is used in the context of naïve T cell activation). **d**) Quantification of the CTV signal dilution factor from (**c**). The CTV signal dilution factor was calculated using the geometric mean of the CTV signal from each population. **e, f**) Transduced T cells were incubated in the indicated metabolic conditions for 18 h before stimulation with PMA/ionomycin for an additional 4 h. The supernatants were then collected for measurement of cytokines. Data shown in **d-f** are from technical replicates (n=3) of one experiment and are representative of at least two independent experiments.

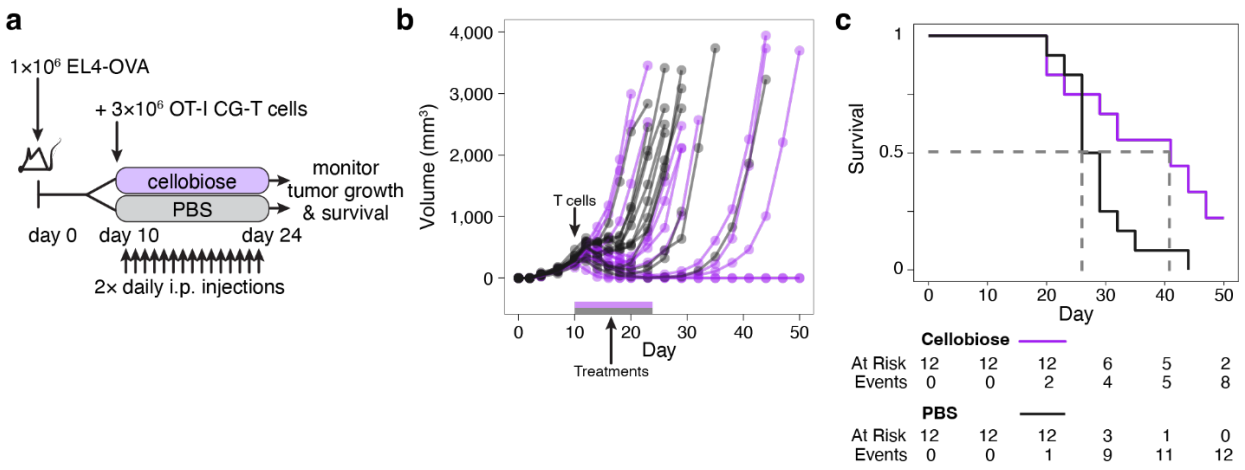

Fig. 4. **T cells that can metabolize cellobiose are a more effective treatment for cancer. a**) Schematic for the cancer experiments. **b**) Tumor volumes for mice receiving T cells on day 10 and twice daily i.p. injections of cellobiose (n=12) or PBS (n=12). Survival was defined by tumors reaching a size cutoff (see Methods). **c**) Survival curves show median survival after transfer with T cells of 31 days for mice treated with cellobiose and 16 days for mice treated with PBS. Two of twelve mice treated with cellobiose showed a complete response. This experiment is representative of two.

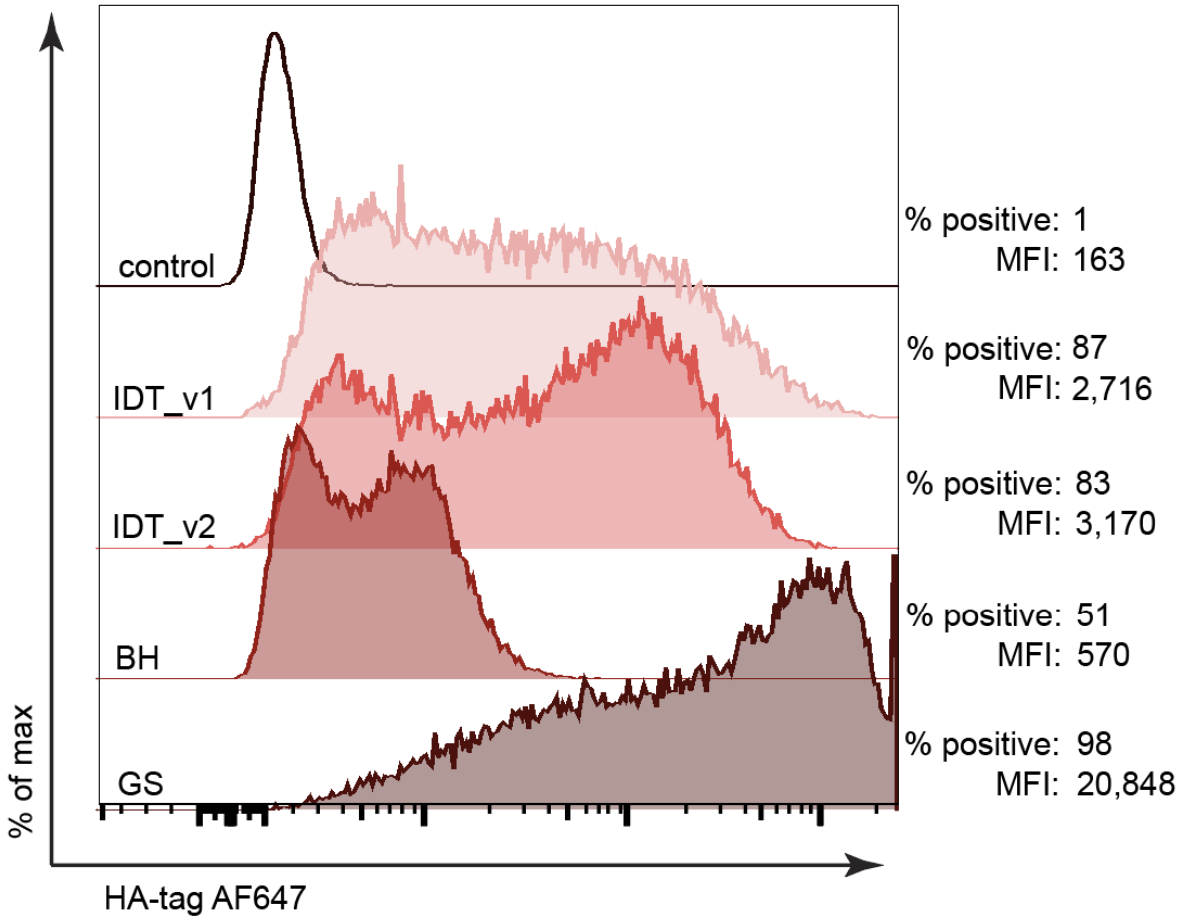

Supplemental Figure 1 | Codon optimization approaches for CDT-1 expression. To generate codon sequences for mammalian expression of CDT-1, we employed publicly available codon optimization algorithms from Integrated DNA Technologies (IDT), Blue Heron Biotech (BH), and GenScript (GS). The sequences were cloned into an MSCV expression vector and transfected into Platinum-E (HEK 293T) cells. After 48 hr, the cells were harvested, fixed, permeabilized, and immunostained for the addended HA-tag. The sequence generated by the GenScript codon optimization algorithm led to the highest expression of CDT-1.

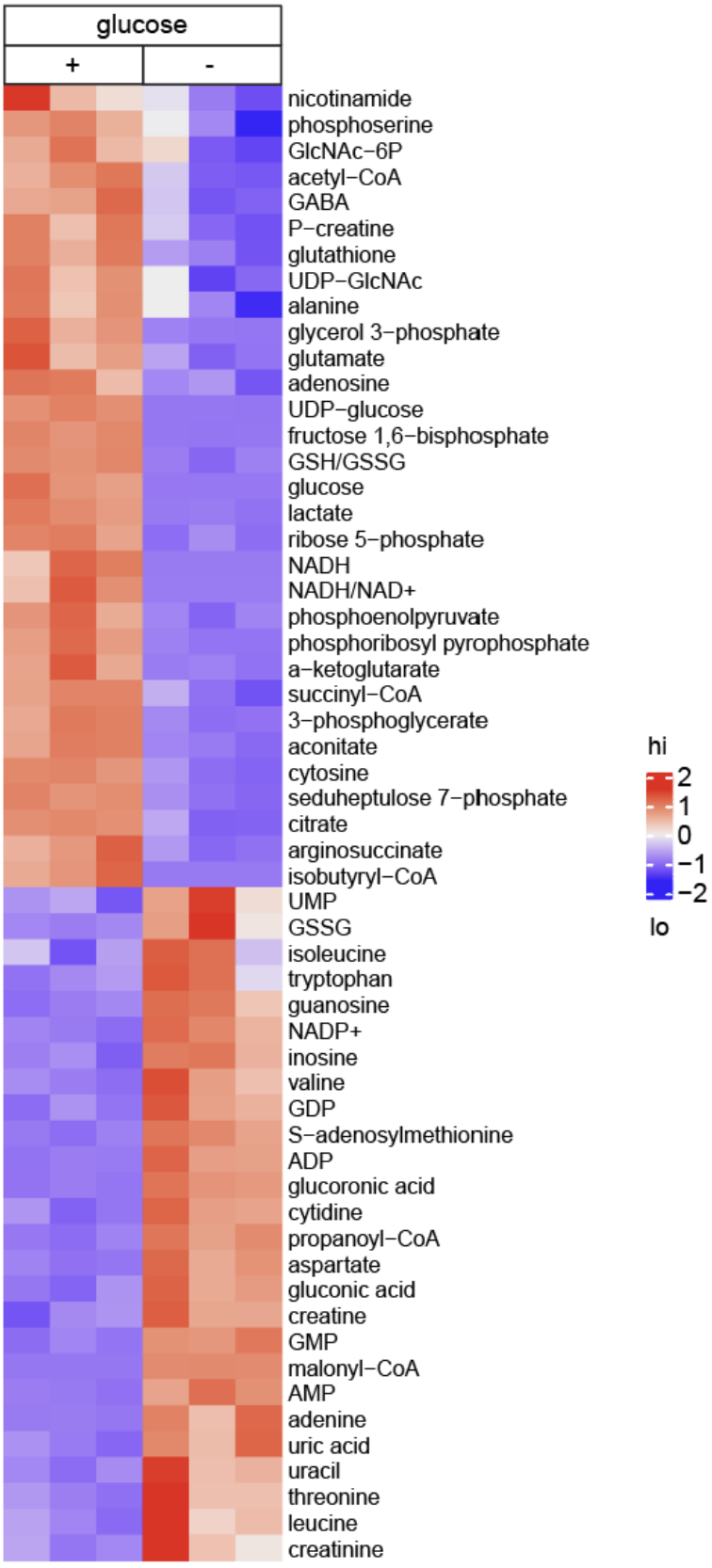
glucose
+
-
nicotinamide
phosphoserine
GlcNAc−6P
acetyl−CoA
GABA
P−creatine
glutathione
UDP−GlcNAc
alanine
glycerol 3−phosphate
glutamate
adenosine
UDP−glucose
fructose 1,6−bisphosphate
GSH/GSSG
glucose
lactate
ribose 5−phosphate
NADH
NADH/NAD+
phosphoenolpyruvate
phosphoribosyl pyrophosphate
a−ketoglutarate
succinyl−CoA
3−phosphoglycerate
aconitate
cytosine
seduheptulose 7−phosphate
citrate
arginosuccinate
isobutyryl−CoA
UMP
GSSG
isoleucine
tryptophan
guanosine
NADP+
inosine
valine
GDP
S−adenosylmethionine
ADP
glucoronic acid
cytidine
propanoyl−CoA
aspartate
gluconic acid
creatine
GMP
malonyl−CoA
AMP
adenine
uric acid
uracil
threonine
leucine
creatinine
hi
2
1
0
−1
−2
lo

Supplemental Figure 2 | Glucose deprivation leads to profound metabolic disturbances in T cells. Activated T cells were cultured with and without glucose for 16 hr and analyzed by LC-MS. T cells deprived of glucose showed depletion of key nutrients in the glycolytic, pentose phosphate, glycosylation and TCA pathways. T cells deprived of glucose accumulated low-energy and oxidative intermediates including AMP and oxidized glutathione (GSSG).

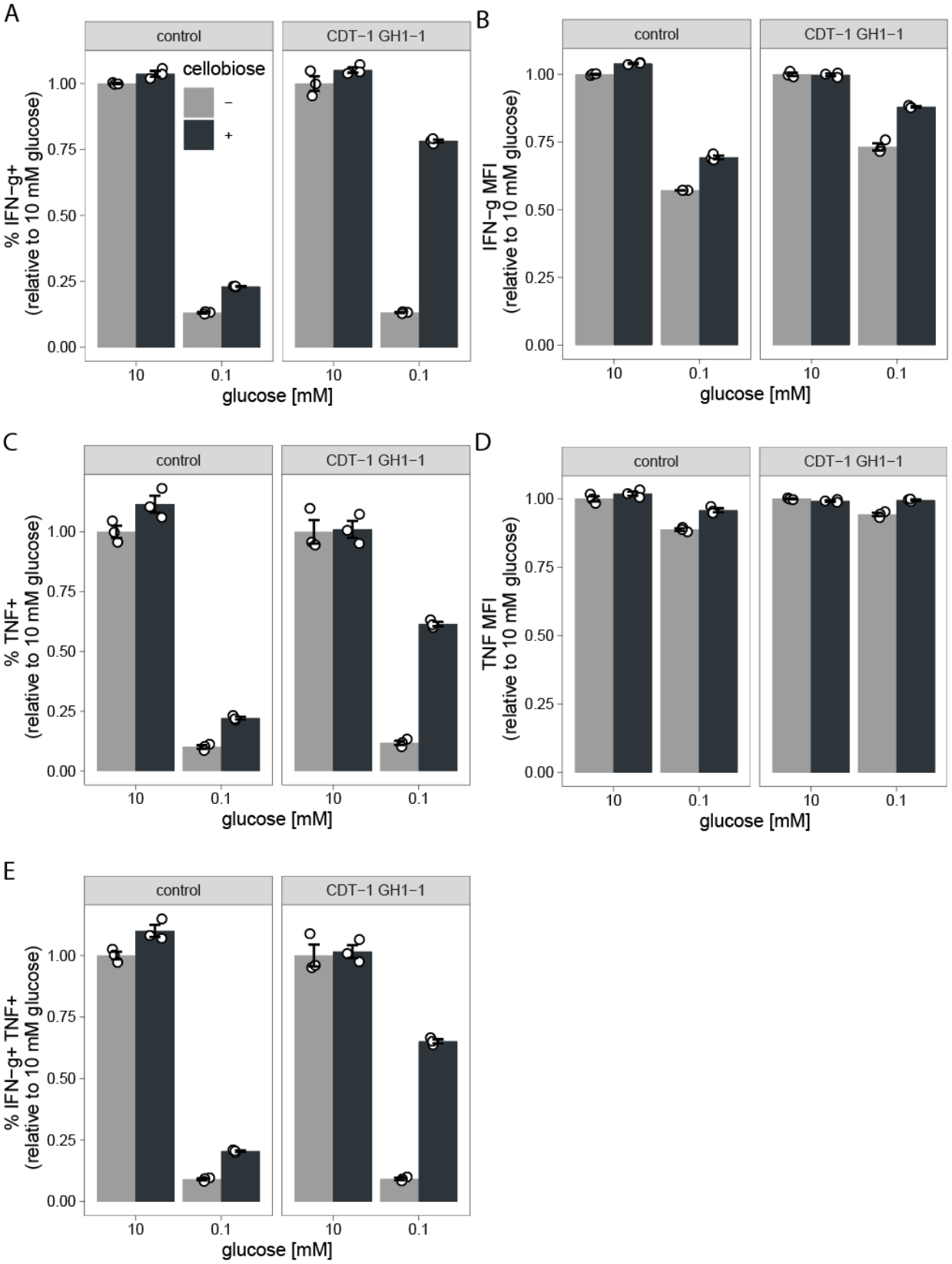
A
control
CDT−1 GH1−1
cellobiose
−
+
% IFN−g+
(relative to 10 mM glucose)
1.00
0.75
0.50
0.25
0.00
10
0.1
glucose [mM]
B
IFN−g MFI
C
% TNF+
D
TNF MFI
E
% IFN−g+ TNF+

Supplemental Figure 3 | Cellobiose rescues intracellular cytokine levels in glucose-deprived CG-T cells. Control and CG-T cells were incubated for 16 hr in the indicated metabolic conditions before stimulation with PMA/ionomycin in the presence of Brefeldin A. The cells were then fixed, permeabilized, and stained to measure the level of intracellular cytokines. The percentages of cells expressing IFNγ and TNF were increased by cellobiose in CG-T cells, but not control cells.

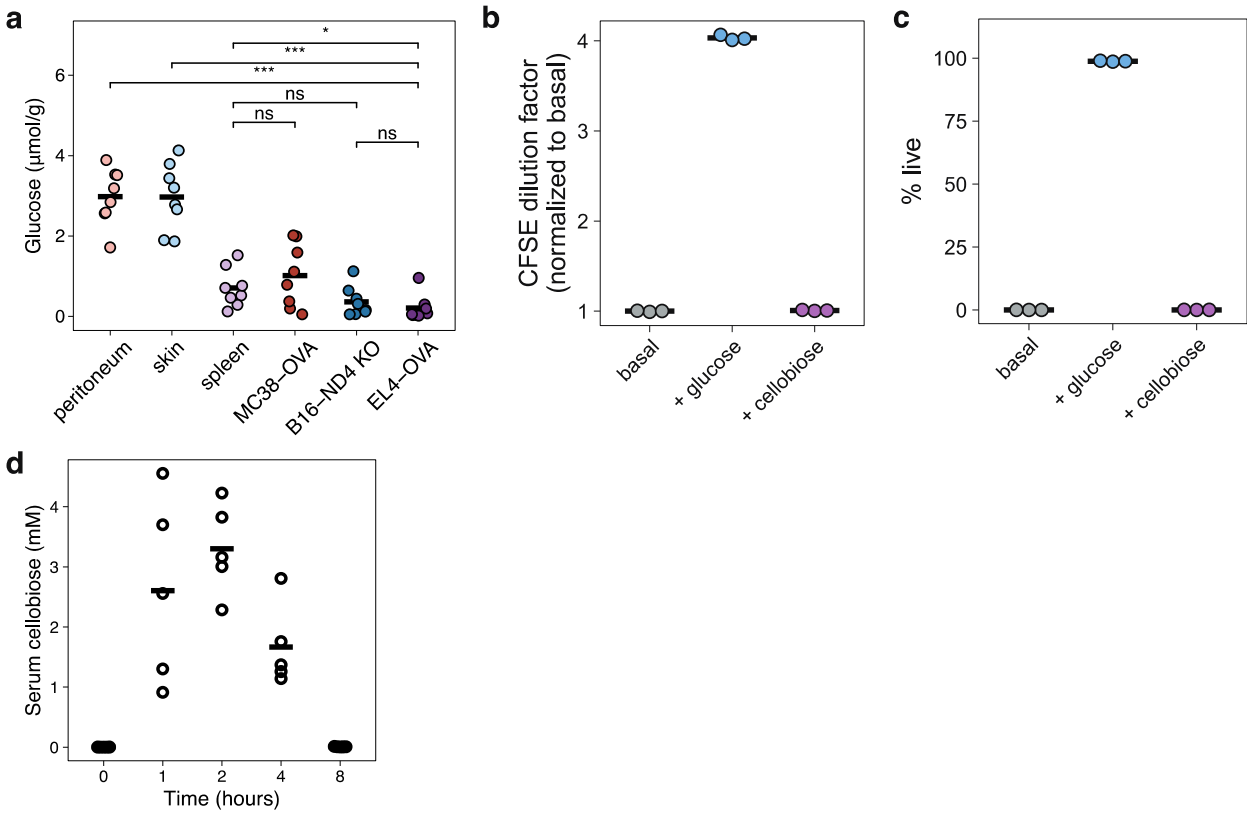

Supplemental Fig. 4. Tumors cannot metabolize cellobiose and pharmacokinetics. a) Tumors and healthy tissues measured for glucose levels by LC-MS. **b)** Proliferation of EL4-OVA tumors cultured with media deprived of glucose (basal), with glucose and with cellobiose. More CFSE dilution indicates more proliferation. **c)** Survival of EL4-OVA tumors cultured with media deprived of glucose (basal), with glucose and with cellobiose as measured by flow cytometry. **d)** Serum concentration of cellobiose at various timepoints after i.p. injection of 85 mg of cellobiose (n=5). Statistical significance in (**a**) was assessed using an unpaired t-test in (*$p < 0.05$; **$p < 0.01$; ***$p < 0.001$; NS > 0.05).

DISCUSSION

Engineered T cells (e.g., CAR-T) already play a major clinical role in fighting lymphomas. In contrast, engineered T cells have struggled to make clinical headway against solid tumors. In the solid TME, TILs (including endogenous and engineered T cells) may be directed to the correct targets but are outcompeted by the tumors for a limited supply of glucose, resulting in a stunted anti-tumor response. The upregulation of glucose transporters such as GLUT1/4 and the kinase HK2 in solid tumors result in the voracious uptake of glucose, sequestering this important nutrient away from the extracellular space[14]. Diminishment of glucose at the tissue scale in tumors can exceed ten-fold compared to healthy, adjacent tissues[54], as our own results substantiated. The impact on the immune response is profound: GLUT1 expression in human tumors negatively correlates with CD8+ T cell infiltration[105]. By engineering the ability to metabolize the natural glucose disaccharide cellobiose into antigen-specific T cells, we present a complementary approach that offers the potential to augment cancer immunotherapies like CAR-T cells in their fight against solid tumors.

There are multiple mechanisms by which provision of glucose enhances T cell responses. Glycolysis fuels the biosynthesis of nucleic acids, lipids, and amino acids. These anabolic processes are critical for cellular maintenance, cytokine production, and proliferation. We showed that carbons derived from cellobiose in our engineered T cells precisely fill those biosynthetic pathways in the absence of other sources of glucose. Deprivation of glucose inhibits expression of IFNγ in effector T cells through regulation at the epigenetic, transcriptional, and translational levels. For example, high concentrations of acetyl-CoA (which can be formed from pyruvate, a product of glycolysis) increase histone acetylation, promoting transcription of proinflammatory genes like *Ifng* and *Tnf* [90]. Additionally, certain glycolytic metabolites, like glyceraldehyde-3-phosphate, can indirectly modulate T-cell function by sequestering GAPDH away from the 3'UTR of the *Ifng* gene. This diversion releases suppressive post-transcriptional control over

translation[89]. These effects are important for anti-tumor immunity, and our results confirmed that production of IFNγ in engineered T cells is rejuvenated by cellobiose in glucose-restricted conditions.

The capacity to metabolize cellobiose has potential for diverse applications. Engineering microbial cells to break down cellobiose has been explored in industrial contexts[122], and can be used for the selection of stably transduced cell lines[147]. The ability to use cellobiose as a glycolytic fuel coupled with isotopically labeled cellobiose is also a powerful tool that researchers can use to tease apart the metabolic dynamics between cells in mixed populations. For example, if tumor cells were enabled to metabolize cellobiose and co-cultured with T cells in the presence of isotopically labeled cellobiose, it might be possible to explore which cellobiose-derived (and by virtue glucose-derived) metabolites the tumor cells were producing that accumulate in and affect T cells (S. Kaech, personal communication). Another application of this work could offer cellobiose to not only enhance but also regulate the vigor of CAR-T cell responses. Many CAR-T cell responses in lymphomas are overactive in the first week and result in morbidity and mortality due to cytokine-release syndrome. If CAR-T cells fueled by cellobiose were to become overactive, the cellobiose infusions could be reduced to curtail cytokine production. Beyond cancer immunology, we believe this approach could be used to answer questions about the regulation of glucose metabolism across many cell types, biological processes, and diseases.

Acknowledgments

We thank Dr. Erika Pearce for her gift of the EL4-OVA cell line. We thank Dr. Greg Delgoffe for advice and for his gift of the B16-ND4 KO cell line. We thank Michael Trump and Humza Khan for assistance with pilot experiments, and other members of the Butte lab for support. We thank Johanna ten Hoeve for her assistance with LC-MS through the UCLA Metabolomics Core. We appreciate the services of LumiGenics LLC for assistance with in vivo metabolite quantification.

Funding

This project was partially funded by the E. Richard Stiehm Endowment (MJB); UCLA Jonsson Comprehensive Cancer Center Fellowship (MLM); National Institutes of Health Ruth L. Kirschstein National Research Service Award GM007185 (MLM); National Institutes of Health grant R21 AI166551 (MJB)

Author contributions:

Conceptualization: MLM, MJB

Investigation: MLM, RN, TJT

Visualization: MLM, MJB

Funding acquisition: MLM, MJB

Supervision: MJB

Project administration: MJB

Writing – original draft: MLM, MJB

Writing – review & editing: MLM, RN, TJT, MJB

Competing interests: The Regents of the University of California have applied for a patent on this work (application # PCT/US22/24298). The authors declare no other competing interests.

METHODS

Mouse lines

Mouse strains were obtained from The Jackson Laboratory: C57BL/6J (JAX 000664) and MHC class I-restricted, $OVA_{257-264}$-specific TCR transgenic (OT-I, JAX 003831). OT-I male mice were bred with C57BL/6J females and females of the F1 generation were used in all studies where OT-I mice were specified. All mice were bred and maintained under specific pathogen-free standards by the Division of Laboratory Animal Medicine at UCLA. All mouse experiments were carried out in compliance with UCLA's institutional policy on humane and ethical treatments of animals following protocols approved by the UCLA Animal Research Committee.

Virus production

To begin viral production, 1×10^6 Platinum-E cells (Cell Biolabs) were plated into 6-well plates in 2 mL DMEM supplemented with 10% heat-inactivated FBS (antibiotics were omitted from this media to increase transfection efficiency and reduce toxicity) and incubated in a humidified chamber at 37 °C, 5% CO2. 24 hr later, Lipofectamine 3000 (Thermo Fisher Scientific) was combined with 400 femtomoles (~2.5 µg) of plasmid according to manufacturer instructions and added dropwise to the well before returning to the incubation chamber. The next morning, the media was aspirated and replaced with 2.5 mL fresh media and returned to the incubation chamber. 24 hr later, the media was harvested, and spun at 500 × *g* for 5 min (to remove cellular contamination). To generate media for co-transduction of two viruses when combined with target cells, supernatants from both control conditions were combined (empty vector-mCherry + empty vector-GFP). Similarly, supernatants from both transgenic conditions (CDT-1 + GH1-1) were combined. Viral supernatants were loaded into Amicon Ultra-Centrifugation Filters with a 100k Dalton molecular weight cut-off (Millipore Sigma) before spinning at 1,000 × *g* for 20 min to

concentrate. The ~200 µL of viral media generated from concentration was then brought up to 1 mL using complete T cell media containing 2 µg/mL of soluble anti-CD28 and 50 U/mL of hrIL-2. 12-well non-tissue culture treated plates were coated with 20 ng µL-1 RetroNectin (Takara Bio). The 1 mL of viral media was then overlaid into these wells and centrifuged at 1,000 × *g* for 90 min. To increase transduction efficiency, viral media was left in the wells before overlaying T cell suspensions. To further ensure high levels of transduction efficiency, viral supernatants were always used for transduction on the same day that the supernatants were harvested.

Primary T cell culture, transduction, and expansion

$CD8^+$ T cells were isolated from the spleens and inguinal lymph nodes of female mice between the ages of 8-12 weeks old using an EasySep immunomagnetic negative selection enrichment kit (Stem Cell Technologies). Complete T cell media for our experiments comprised RPMI-1640 supplemented with 10% heat-inactivated FBS, 100 U/mL penicillin/streptomycin, 1 mM sodium pyruvate, 10 mM HEPES buffer, and 0.1% β-mercaptoethanol. Tissue culture-treated 12-well plates were coated with 10 µg/mL anti-CD3 (clone 2C11; BioXCell) overnight at 4 °C then washed. T cells were activated by resuspending at a density of 2×10^6 cells/mL in media additionally containing 2 µg/mL of soluble anti-CD28 (clone 37.51; BioXCell) and 50 U/mL of hrIL-2 (BRB Preclinical Repository, National Cancer Institute, NIH); 1 mL was plated onto each well, and then incubated in a humidified chamber at 37 °C, 5% CO_2. After 24 hr, T cells were harvested, and supernatant was collected and saved at 4 °C. T cells were resuspended in an equal volume of fresh complete T cell media with 2 µg/mL soluble anti-CD28 and 50 U/mL hr of IL-2 and 1 mL of suspension was overlaid onto virus-loaded plates (see Virus production above). T cells were "spinfected" by centrifuging the plates at 1,000 × *g* at 32 °C for 90 min. Then the plates were transferred into the 37 °C incubator for an additional 90-min incubation. The viral media was then carefully removed, leaving behind the adherent T cells, before adding back 1 mL of the previously

stored supernatant from overnight activation in addition to an extra 1.5 mL of fresh complete T cell media supplemented with 2 μg/mL of soluble anti-CD28 and 50 U/mL of hrIL-2. Transduced T cells were incubated overnight. The next morning, T cells were harvested and transferred into 15 mL of fresh complete T cell media supplemented with 50 U/mL of hrIL-2 before incubating at 37 °C for another 24 hrs. The following morning, T cells were harvested and resuspended in fluorescence associated cell sorting (FACS) buffer (composed of Dulbecco's Phosphate Buffered Saline supplemented with 2% FBS and 1 mM EDTA) and sorted using a Sony SH800S flow cytometric sorter. Post-sorting expansion involved daily passaging of T cells into fresh complete T cell media, expanding the total culture volume 4-fold with each daily passage. All experiments were performed on cells 5-7 days after activation.

Expression cassette design and construction

To generate the control viral vectors, a plasmid containing the mouse stem cell virus (MSCV) backbone (Addgene #24828) was modified to introduce new expression cassettes containing the desired promoter, cloning site, fluorescent reporter, and regulatory element (**Fig. 1a**). First, the viral cargo between the truncated gag and 3' long terminal repeat (LTR) was removed by amplifying the plasmid backbone, using Phusion polymerase (Thermo Fisher Scientific) and the primers 5'-GGCGCCTAGAGAAGGAGTG-3' and 5'-ATGAAAGACCCCACCTGTAG-3'. The PCR product was then combined with separate gBlocks Gene Fragments (Integrated DNA Technologies) containing the new expression cassettes and assembled with NEBuilder HiFi DNA Assembly Master Mix (New England Biolabs).

To generate the transgenic viral vectors, the amino acid sequences for cdt-1 (KEGG ID NCU00801) and gh1-1 (KEGG ID NCU00130) were codon optimized for murine expression using the GenSmart Codon Optimization Tool (GenScript) and constructed as gBlocks Gene Fragments (Integrated DNA Technologies) with 25 base pair overlaps at the 5' and 3' ends that provided

homology to the control plasmids after digestion with NotI and BamHI. All plasmid constructs used in this study will be made available through Addgene.

Metabolite extraction

For cells in suspension: cells were harvested, pelleted at 500 × *g* for 60 sec, and washed with ice-cold PBS before adding 1 mL of a mixture of 40:40:20 methanol:acetonitrile:water to each cell pellet. Each sample was then spiked with 1 nmol of Norvaline (Millipore-Sigma) before vigorously vortexing for 30 sec. Samples were then placed at -20 °C for 1 hr to aid extraction/ protein precipitation and then again vortexed for 30 sec at the end of the extraction incubation. Samples were then spun at 16,000 × *g*, 4 °C for 10 min to pellet cellular debris. Equal volumes (~900 µL) of supernatants were then transferred into glass vials before drying in an EZ-2 Elite (GeneVac) for 60 min. To determine the cell pellet protein content for normalization, the cell pellet was lysed with 0.2 M NaOH, heated to 95 °C for 20 min, and then quantified using a Pierce BCA assay (Thermo).

For tissues: ~25 mg of flash frozen tissue was added to a microcentrifuge tube containing a 5 mm grinding ball (440C Stainless Steel, OPS Diagnostics) and 1 mL of an mixture of 80:20 methanol:water. The tissues were then homogenized on a TissueLyser II (Qiagen), using 30 oscillations/sec in pulses lasting 30 sec until the tissue was homogenously broken down. The pellets were then incubated at -80 °C for 1 hr to aid extraction and protein precipitation, and then vortexed for 30 sec. Samples were then spun at 16,000 × *g*, 4 °C for 10 min to pellet cellular debris and a volume corresponding to 5 mg of tissue was transferred into a glass vial before drying in an EZ-2 Elite to evaporate the fluid.

Metabolomics

Dried metabolites were resuspended in 50% acetonitrile (ACN) in water, and an aliquot was loaded onto a Luna 3 µm NH2 100 A (150 × 2.0 mm) column (Phenomenex). The chromatographic separation was performed on a Vanquish Flex (Thermo Scientific) with mobile phases A (5 mM NH4AcO pH 9.9) and B (ACN) and a flow rate of 200 µL/min. A linear gradient was run from 15% A to 95% A over 18 min and was followed by 7 min isocratic flow at 95% A and re-equilibration to 15% A. Metabolites were detected with a Thermo Scientific Q Exactive mass spectrometer run with polarity switching (+3.5/−3.5 kV) in full scan mode with an *m/z* range of 70–975. The open source Maven (v 8.1.27.11) application was used to quantify the targeted metabolites by area under the curve using expected retention time and accurate mass measurements (<5 ppm). The cell culture experiments were normalized to protein content. The tissue experiments were normalized to tissue content (weight). Data analysis was performed using in-house R scripts (https://github.com/graeberlab-ucla/MetabR).

Microscopy

Wells of Nunc Lab-Tek II Chambered Coverglass (Thermo Fisher) were coated with 100 µg/mL poly-d-lysine in PBS, incubated at 4 °C overnight, aspirated, and allowed to air dry. 50,000 cells in 200 µL complete T cell media were gently overlaid in a well of the chamber and allowed to settle in a humidified, 5% CO_2 chamber at 37 °C for 1 hr. The cells were then washed with PBS and then incubated at room temperature for 30 min with a 4% paraformaldehyde in PBS solution. After two washes with PBS, the cells were incubated with intracellular staining permeabilization wash buffer (BioLegend) for 5 min at room temperature before blocking for 60 min at room temperature using 10% donkey serum diluted in permeabilization buffer. After blocking, the cells were incubated in permeabilization buffer with a 1:200 dilution of anti-HA-tag (clone 16B12,

BioLegend) conjugated to Alexa Fluor 647 for 60 min at room temperature. The cells were washed twice with permeabilization buffer, and a third time with PBS, before overlaying Fluoromount-G Mounting Medium with DAPI (Invitrogen). The cells were imaged at 100× magnification using a Ti ECLIPSE (Nikon) microscope, modified with a CSU-X1 (Yokogawa) confocal scanner unit and a XR/MEGA-10 (Stanford Photonics) camera. Images were acquired using MicroManager and analyzed in Fiji.

Glucosidase activity assay

T cells were lysed using Pierce IP Lysis buffer (Thermo) supplemented with Halt protease inhibitor cocktail (Thermo), incubated on ice for 10 min with periodic vortexing, and centrifuged at 15,000 × *g* at 4 °C for 15 min. The protein concentration of the supernatant was then quantified using a Pierce BCA assay (Thermo). 10 µL of lysate (corresponding to 50 µg of protein) was then combined with 10 µL cellobiose (final concentration of 1 mM), and 30 µL of reaction buffer (50 mM phosphate buffer, pH 6.0)[148] before overlaying 50 µL of working reagent from a glucose detection assay (Amplex Red Glucose/Glucose Oxidase Assay Kit, Invitrogen). Glucose production and oxidation was detected using a Biotek Cytation5 plate reader to measure absorbance at ~560 nm over time.

Proliferation assay

Transduced T cells were stained with 1 µM CellTrace Violet (Thermo Fisher) reagent in PBS with 0.1% BSA and incubated for 15 min at 37 °C with regular agitation. Staining was neutralized with complete T cell media before pelleting cells and resuspending in basal media for metabolic assays, composed of RPMI 1640 minus glucose supplemented with 10% dialyzed, heat-inactivated FBS (Thermo Fisher), 100 U/mL penicillin/streptomycin, 10 mM HEPES buffer,

0.1% β-mercaptoethanol, and 50 U/mL of hrIL-2. An equal volume of basal media supplemented with 2x glucose or cellobiose concentrations was then overlaid to achieve the desired 1x concentration for glucose or cellobiose. The cells were incubated in a humidified chamber at 37 °C, 5% CO_2 for 48 hr before harvesting for CTV signal analysis on a SH800S (SONY) cell sorter.

Cytokine production assay

Transduced T cells were incubated for 18 hr in basal media (composed of RPMI 1640 minus glucose supplemented with 10% dialyzed, heat-inactivated FBS (Thermo Fisher), 100 U/mL penicillin/streptomycin, 10 mM HEPES buffer, 0.1% β-mercaptoethanol, and 50 U/mL of hrIL-2) plus or minus the indicated concentrations of glucose or cellobiose. To measure cytokine in the supernatant, the cells were then stimulated with PMA (40 ng/mL) and ionomycin (1 μM) for 6 hr, then supernatants were diluted before quantification of cytokines by Cytokine Bead Array (BD Biosciences), following the manufacturer instructions. To measure cytokine production on a per-cell basis, the cells were stimulated with PMA (40 ng/mL) and ionomycin (1 μM) in the presence of Brefeldin A (5 μg/mL) for 6 hr. T cells were then fixed in 2% paraformaldehyde and 5% sucrose solution for 20 min at room temperature, before permeabilization and staining for intracellular cytokines, and measurement on a flow cytometer.

EL4-OVA tumor model

For tumor experiments, cohorts of female C57BL/6J mice born on the same day and between 9-11 weeks old were used. The physical health and behavior of mice were monitored daily to ensure that they did not lose more than 20% of starting weight, did not show signs of stress, and could continue to feed and drink uninhibited. The mice were injected subcutaneously in the flank with 1×10^6 EL4-OVA tumor cells on day 0. The tumors were allowed to grow until day

8, then the mice were re-asssorted into two groups such that the average size of the tumors was the same in both groups. The mice then underwent i.v. injection of 3×10^6 OT-I CG-T cells. Then the mice were injected twice daily with cellobiose 85 mg i.p. or PBS in the same volume in a blinded fashion until day 22. Tumor sizes continued to be followed until the endpoint. The endpoint for each mouse was determined based on physical health, tumor ulceration (which did not occur for EL4-OVA), or if the tumor exceeded 20 mm in diameter in any dimension, or the average of the tumor length or width exceeded 17.5 mm. Tumor volumes were calculated as $4/3 \times \pi \times [(L+W)/2\ ]^3$, where L and W are the measurements of length and width by calipers. Thus, the survival cutoffs we used correspond to large tumors, volumes between 2000-4000 mm^3. Statistical comparisons were done using the R package survival, using the Cox regression command coxph using a volume of 2200 mm^3 as a cutoff.

CHAPTER 5

FUTURE DIRECTIONS

The in vitro experiments performed in this work have demonstrated that, in the context of a glucose depleted environment, granting activated T cells a renewed ability to fuel glycolysis can robustly rescue effector functions including survival, proliferation, and cytokine production. It should be noted that the rescues using cellobiose did not reach 100% of the levels demonstrated in the full glucose controls. As metabolite tracing revealed nearly identical use of cellobiose carbons compared to glucose carbons, the most likely cause of incomplete rescue is suboptimal expression levels and functionality of the cellobiose catabolism proteins, CDT-1 and GH1-1. In experiments testing single and doubly transduced cells (GH1-1 only vs CG-T cells), GH1-1 T cells nearly reach the performance of CG-T cells (data not shown), indicating that addition of the transporter is not yielding significant improvements over cells expressing the hydrolase alone. Additionally, while the CDT-1 cellobiose transport experiments did show significance in the intended functionality of the transporter, the magnitude of transport was not a great deal higher than non-transduced controls (2x difference after 125 minutes).

Future work should focus on improving the functionality of the cellobiose transporter protein to increase the rate of cellobiose transport into the cell, thereby allowing cellobiose supplementation to further increase the rate of T cell glycolysis during glucose withdrawal. During immunoblot characterization of CDT-1, the transgenic protein consistently appeared at a lower molecular weight than predicted and as a doublet. Shifts in molecular weight may be explained by post-translational modifications, such as phosphorylation or glycosylation, but these modifications normally increase molecular weight, which may be relevant in the generation of the observed doublet. Proteins appearing at lower molecular weights may be due to incomplete translation. In our case, the HA-tag epitope used to modify CDT-1 for immunostaining analysis was addended to the C-terminus, suggesting that the low molecular weight bands that appear during immunoblot analysis have had translation run through the C-terminus of the transcript.

Several strategies were implemented to improve the function of the transporter CDT-1. Peptide sequences that alter protein trafficking to enforce localization at the plasma membrane[149] were tested, alone and in combination, but yielded no improvement in cellobiose transport capacity (data not shown). Mutant CDT-1 transporters have been reported to enhance cellobiose transport after heterologous expression in *Saccharomyces cerevisiae*[148], but in our hands the reported F213L and G91A mutants resulted in no functional differences to glycolytic rate (data not shown). Finally, orthologs and paralogs, including CDT-2, CDT-2 N306I, CdtC, and CtA[122,127,150,151], were tested and, again, yielded no functional enhancement in the capacity to transport cellobiose when expressed in primary T cells (data not shown).

In vivo application of the cellobiose system towards the enhancement of glucose-deprived, tumor-infiltrating T cells produced significant, but modest increases in survival of tumor bearing mice. **There are many considerations towards the development of a more robust in vivo experimental result.** The primary considerations are the appropriateness of the model itself, the condition of adoptively transferred T cells, and the pharmacokinetics of cellobiose delivery.

For T cells to benefit from cellobiose as a fuel source, cellobiose must be present in the environment at high concentrations. For in vitro assays, cellobiose could be supplied at high concentrations (5-10 mM) and maintained around the desired level throughout the course of any given assay, which produced not only significant results but also large effect sizes. In contrast, in vivo delivery of cellobiose into the bloodstream is significantly more challenging. Since cellobiose is meant to replace glucose as a carbohydrate fuel source, the target for cellobiose concentration in the blood should not only match or approach the concentration of glucose in the blood, which in mice and humans is around ~5 mM, but should also be temporally sustained. While it may be argued that after hydrolysis, one unit of cellobiose provides two units of glucose (and therefore halves the concentration of cellobiose that is needed relative to glucose) the blood concentration of cellobiose would still ideally be maintained in the millimolar range. The cellobiose delivery

strategy implemented in this work relied on repeated intraperitoneal injections of a cellobiose bolus. While the blood concentration after cellobiose injection was demonstrated to reach several millimolar within two hours, it was also clear that the concentration would drop back to nearly zero after just eight hours. As a result, we had to choose a cellobiose administration strategy that involved repeated injections throughout the day. This approach results in a blood cellobiose concentration that spikes into the millimolar range multiple times throughout the day but was most likely in the sub-millimolar range for the majority of the 24 hours cycle. Osmotic pumps were considered as an alternative means of cellobiose delivery, but the rate of diffusion and reservoir capacities are too low to efficiently deliver our desired compound, as it is intended to serve as a fuel source that has extremely high rates of turnover. Adding cellobiose into food and water was also considered (and tested) but resulted in no appreciable accumulation into the blood (data not shown). **Developing a method to improve cellobiose delivery such that cellobiose accumulates in the blood at high concentrations and is sustained throughout a 24-hour cycle could enhance the effectiveness of the treatment.** Of note, application in human therapy could see hospital patients receiving intravenous infusion of cellobiose for several hours throughout the day or continuously over several days, similar to what is currently employed for certain chemotherapies.

A second consideration towards achieving a more robust in vivo result is the relevance of the model system being employed. As discussed in the introduction, tumors may create glucose depleted environments due to their hyperproliferative nature, but the extent to which this happens varies from one tumor type to the next. The tumor models that are available for us to test the cellobiose system are constrained by multiple factors. For adoptive cell therapies, the engrafted cancer cells must express a protein that can produce a neoantigen target for which there is a defined TCR pairing, Ideally, this paired TCR has previously been introduced into a transgenic mouse line. Example antigen/TCR pairings include OVA/OT-I, gp100/PMEL, and gp33/P14. This

constraint significantly limits which cancer cell lines are available to be used in our model system. Among the cancer cells lines that do meet these requirements, we chose three that have been demonstrated to display elevated rates of glycolysis and measured the tissue glucose content within them (EL4-OVA, MC38-OVA, and B16 ND4 KO [which expresses gp100]). As a result of this analysis, we decided to move forward with EL4-OVA (paired with OT-I T cells) as our model system because the tumors developed by EL4-OVA cells were the most glucose deficient.

Another consideration for choosing an appropriate model system is the immunocompetency of the host. When working with mice that have fully intact immune systems, the cancer cell line and tumor host must be syngeneic, lest the engrafted cells be outright rejected by the host. Additionally, immunocompetent mice contain endogenous tumor-infiltrating lymphocytes that may exert outsize influence on tumor trajectories and therefore mask the impact of adoptively transferred cells that are under study[152]. Using immunodeficient mice such as RAG KO mice, which lack mature B and T cells, can allow studies to proceed in the absence of endogenous lymphocytes. Mice with a severely impaired immune system, such as NSG (NOD-scid IL2Rg^{null}) mice that contain no functional B, T, or NK cells, can be used to engraft human cancers, thereby expanding the number of model systems that are available to test our cellobiose system with, so long as there is still an antigen/TCR pairing between the cancer cells and adoptively transferred T cells. NSG mice are particularly useful in the study of CAR T cells, for which many more CARs have been developed against human antigens/targets compared to mouse antigens/targets.

While EL4-OVA tumors did generate glucose depleted environments, we did not produce direct evidence that adoptively transferred, tumor-infiltrating OT-I T cells experience glucose withdrawal to the extent that it detracts from their effector functions during tumor infiltration. Competition for glucose between tumor cells and tumor-infiltrating T cells that results in tumor progression has been demonstrated in the past[143], and is the basis for this work, but the number

of experiments that is required to adequately demonstrate T cell dysfunction as a result of tumor glucose sequestration goes beyond the resources that were available for this work.

Future efforts to identify the ideal model(s) to test our cellobiose system could expand across two fronts. The first would focus on deeper characterization of the extent to which adoptively transferred T cell effector function is hampered by glucose depletion within a given tumor model, and thus provide clearer insights into whether the tested tumor model creates a window for a therapeutic effect for the cellobiose system. The second front would focus on aggregating a large cohort of candidate cancer cell lines (that allow for antigen/TCR pairings of adoptively transferred T cells), empirically testing the engtafted tumors side-by-side for tumor glucose content (rather than relying on external reports of elevated glycolytic features), and selecting the tumor type which generates the most glucose barren tissue. The second approach should be prioritized because it is significantly less resource intensive than the first and would produce an actionable result in a significantly shorter timeframe. If the previously discussed parameters of the cellobiose system are optimized and the approach is still not resulting in a therapeutic effect in those tumors that have been empirically demonstrated to host the lowest glucose contents, then the overall approach to fuel T cells with cellobiose may not be widely applicable as a frontline therapy.

A third variable to consider in the attempt to generate a more robust result from the cellobiose system is the functional state of the adoptively transferred T cells. Endogenous and adoptively transferred TILs exhibit a wide spectrum of phenotypes that correlate with their functionality in the tumor environment. Several lines of study have demonstrated that chronic antigen exposure can lead to elevated expression of programmed cell death protein 1 (PD-1) in T cells, resulting in an “exhausted” state that renders T cells dysfunctional and impaired in their ability to clear tumors and infections[153–155]. Ligation of PD-1 produces a signal transduction cascade that exerts a potent inhibitory influence on cytokine production, cell cycling, and

survival[156]. Importantly, the capacity to carry out glycolysis is also negatively regulated by PD-1 signaling. **PD-1 ligation potently shifts the metabolic program of T cells away from glycolysis** and towards lipolysis and fatty acid oxidation, a process that is partially mediated by a decrease in GLUT1 and HK2 expression[157–159]. There is also evidence that PD-1 signaling abrogates glycolysis in other immune subsets such as monocytes and macrophages[160,161].

In our EL4-OVA/OT-I adoptive transfer model, we extracted TILs on day 6 post adoptive transfer and performed surface staining of PD-1. This analysis showed that between 70-95% of transferred cells were positive for PD-1 (data not shown). It is important to note that beyond chronic antigen stimulation, PD-1 expression also increases after activation and the expression of PD-1 alone is insufficient to conclude that these cells are phenotypically “exhausted”. Regardless, the expression of PD-1 at the cell surface suggests that these cells do maintain the capacity to engage in PD-1 signaling, the magnitude of which would be dependent on the presence of ligands for PD-1 in the environment. Programmed death-ligand 1 (PD-L1) is a high-affinity ligand for PD-1[162] and, due to a large variety of mechanisms that lead to upregulation, can often be found expressed on cancerous tissue[163]. EL4 has been previously demonstrated to express high levels of PD-L1 when cultured in vitro[164], and in our hands, EL4-OVA expressed PD-L1 both as cells grown in culture and when grown as a tumor in vivo (data not shown).

It stands to reason that if PD-1 is present on the surface of adoptively transferred cells and PD-L1 is present on the surface of tumor cells, the interaction of this ligand/receptor pair in the tumor environment may result in PD-1 based inhibition of glycolysis in adoptively transferred cells. Therefore, even if the cellobiose system is optimized to maximize efficiency of transport and hydrolysis of cellobiose and tested in the best model for tumor glucose depletion, PD-1 signaling may inhibit the expression of glycolytic machinery within TILs and prevent glucose produced from cellobiose from being efficiently catabolized. **Therefore, we believe that PD-1 blockade will be an appropriate setting to maximize the benefit of the cellobiose system.**

An important consideration for the implementation of the cellobiose system in the context of PD-1 blockade is the impact that anti-PD-1 therapy may have on endogenous T cells. PD-1 blockade is an effective therapy in its own right, because of the ability to invigorate endogenous T cells. A study of PD-1 blockade in immunocompetent, melanoma bearing mice that received adoptively transferred T cells determined that the observed therapeutic effect was primarily due to PD-1 invigorating the endogenous TILs[152]. Indeed, implementation of PD-1 blockade in our EL4-OVA/OT-I model results in a large fraction of tumors regressing, independent of the number of adoptively transferred T cells (data not shown). Staining of endogenous TILs in this model reveals that, just as in the adoptively transferred T cells, a high fraction of endogenous TILs also show high expression of PD-1 (data not shown). Finally, it is also important to consider that reinvigoration of endogenous TILs from PD-1 blockade may produce a higher concentration of glucose within the tumor environment, due to high levels of cancer cell death and less voracious consumption of glucose[143]. **Given the impact of PD-1 blockade on endogenous TILs, we suggest testing the cellobiose system with anti-PD-1 in the context of immunocompromised hosts, such as Rag1 KO mice.**

CHAPTER 6

CONCLUDING REMARKS

Cancer is marked by an abnormal increase in cell growth, a process frequently supported by a metabolic organization that includes high rates of glycolysis. As a result, tumors often consume abnormal rates of glucose compared to healthy tissue. Consequently, this increased consumption can outpace the resupply of glucose, leading to glucose scarcity in the tumor environment. Our approach aims to take advantage of this common feature of cancer and generate a therapy that is widely applicable in solid tumor settings, which account for over 90% of all diagnoses.

Tumor heterogeneity (both inter- and intra-) that results in different scales of glucose depletion is an important consideration in application of the cellobiose system, as the scale controls the size of the window for a therapeutic effect. How common is it for cancer to be depleted of glucose and to what extent? Multiple methods have been employed to measure the concentration of metabolites in tumors, including: 1) direct sampling of tumor interstitial fluid with microdialysis[165], 2) ex vivo purification of interstitial fluid with centrifugation[166–168], and 3) bulk-tissue analysis[54]. Due to technical variability between approaches, intrinsic biological variability (i.e. tissues of origin, oncogenic driver mutations etc.), and a relatively limited number of tumor metabolomics studies that have been conducted, few metabolites have been identified that are consistently differentially enriched or depleted in tumor tissue compared to healthy tissue. Meta-analysis of these studies has concluded that among those that are consistently different, glucose is the first or second most commonly depleted metabolite measured across tumor environments[169,170]. Thus, it appears that a large fraction of tumors (and perhaps most) consume glucose at a rate that outpaces perfusion, resulting in a glucose-depleted tumor microenvironment[171]. The extent of glucose depletion that may be produced in the tumor environment appears variable, with results ranging from insignificant[165,172] to over 10-fold decreases[54–56,143,173]. With further refinement, the cellobiose system may be able to provide a

therapeutic effect when tumor glucose levels are marginally depleted, but, in the current state, is likely to show a benefit only when tumor glucose depletion is more extreme.

While the detrimental effect of glucose depletion on immune function in the tumor environment has been extensively investigated and reported on, the frequency and impact of nutrient competition in the tumor environment has been called into question. Recent work has demonstrated in both mouse and human tumors that glucose may be present in appreciable quantities in the tumor environment[170,172,174,175] and therefore non-limiting for TIL function. It has also been observed in a mouse and human tumor cell model that, on a per cell base, tumor infiltrating myeloid cells consume more glucose than the cancer cells themselves, and in total, accounted for roughly 1/3 of the tumor glucose consumption[175]. This observation may suggest that glucose is available for immune consumption, but does not preclude the possibility that, in addition to cancer cells, TILs are also in competition with other immune subsets, resulting in an inadequate supply of glucose to achieve maximal effector function. More relevant is the finding that inhibition of glutamine uptake increases glucose uptake in all tumor cell populations, suggesting that glutamine metabolism restrains glucose metabolism and that tumor infiltrating cells can increase glucose uptake beyond basal levels when glutamine is restricted[175]. This finding may suggest that glucose uptake is cell-intrinsic and not based on environmental levels, but was not definitively demonstrated because glucose levels in the tumor environment were not directly measured with and without glutamine inhibition. It may be argued that the insult that tumor and tumor-associated cells receive to metabolism, growth, and proliferation during glutamine inhibition may concomitantly stunt overall glucose uptake, increasing glucose levels in the tumor environment, and allowing for increased glucose uptake compared to no treatment controls.

Tumor perfusion significantly impacts the consistency and magnitude of tumor glucose depletion and can be leveraged to guide clinical application of the cellobiose system. Compared to healthy, well-perfused tissue, poorly perfused tumors/tumor regions engage in higher rates of glycolysis and produce lower concentrations of environmental glucose[176]. Dynamic contrast enhanced-magnetic resonance imaging (DCE-MRI) is a relatively cheap, non-invasive means to assess tumor perfusion that can be used to identify the patients with greatest potential for therapeutic efficacy from the cellobiose system[176,177]. Fluorodeoxyglucose-18 positron emission tomography ([^{18}F]FDG-PET), which can assess total lesion glycolysis[178], could offer a complimentary approach to stratify patients by determining which tumors are relatively elevated in glycolysis and thus most likely to host the low concentrations of interstitial glucose.

The cellobiose catabolism genes, cdt-1 and gh1-1, are derived from microbial sources and, when introduced into mammalian systems, generate the potential for immunogenicity. This problem has recently gained more widespread attention in the use of CAR-T cells[179] for cancer therapy, and is due to the inclusion of mouse components in the CAR constructs, as well as the generation of novel peptide sequences where CAR components (i.e. intracellular signaling domains and short chain variable fragments) are fused together. Regardless of the potential for immunogenicity, CAR-T cells have achieved remarkable clinical successes and are currently employed in over 1,000 clinical trials in the U.S[180]. It should be noted that immunogenicity is likely to be a more significant factor for cellular therapies containing non-human proteins that are administered as multiple doses, and may be minimized through lymphodepletion before the administration of the first dose[181]. If immunogenicity is identified as posing a significant barrier to implementation of the cellobiose system, it may be possible to redirect or broaden the substrate specificity of human proteins to enable cellobiose hydrolysis and transport[182]. For example, the enzyme lactase is a β-glucosidase that efficiently cleaves the β-1→4 glycosidic linkage found in

lactose (a disaccharide of glucose and galactose). Directed evolution[130,183–185] of lactase could be used to broaden its specificity to include cellobiose, enabling cellobiose hydrolysis with significantly lower potential for immunogenicity.

Ideally, the cellobiose system will eventually be incorporated into CAR-T cell production pipelines and tested in pre-clinical trials, but in its current state, the approach requires further refinement and proof of principle. Much of the feedback we have received concerns demonstration of the cellobiose system in the context of CAR-T cell models, which is certainly an exciting prospect, but is not strictly necessary in our quest to more convincingly demonstrate the utility of the cellobiose system to enhance glycolysis in TILs. Currently, co-transduction efficiency of cdt-1 *and* gh1-1 is inefficient (<5%) and requires enrichment via the expression of two fluorescent proteins (mCherry and GFP, respectively). The addition of a CAR gene transduction into the generation and enrichment of CG-T cells complicates the production pipeline because it would require co-transduction and selection of a third transgene. Using a model that involves CAR/antigen pairing is an unnecessary complication because it provides no advantage over TCR/antigen pairing in demonstrating our proof of principle, while also limiting the number of potential tumor models that could be used (i.e. only those which express an antigen that is recognized by existing CAR constructs). Rather than focusing on producing exciting results from the system in CAR-T cells, near term efforts should focus on improving the efficiency and efficacy of the cellobiose system in the models that contain the largest therapeutic window and allow for the greatest size of a therapeutic effect (i.e. in tumors that create an extreme glucose deficiency that has a large detrimental effect on TIL effector function).

While the application of the cellobiose system towards cancer immunotherapy is an exciting prospect, the system has high potential to prove useful in disparate contexts. In 2022, a research group developed a selection system (coined “Celloselect”), wherein the transduction of cell line by two viruses containing cdt-1, gh1-1, and a third gene of interest (GOI) allowed for selection of the successfully transduced cells when glucose was withdrawn and cellobiose supplemented in[147]. Over time, cells that were not successfully co-transduced died, due to the absence of glucose, while those that received cdt-1 and gh1-1 would survive through their capacity to metabolize cellobiose. The surviving cells also stably expressed the GOI. This system allows for cell lines transduced with a GOI to be selected for in the absence of toxic chemicals (i.e. antibiotics) that could negatively impact the scale of production of the GOI, a problem in the large-scale production of certain monoclonal antibodies[186].

An alternative application of exclusive cellobiose metabolism was devised in the lab of Dr. Susan Kaech (who is also interested in the metabolic interactions of cells within the tumor environment), wherein the cellobiose system could be used to identify metabolites that are exchanged between cancer cells and other cells in the tumor environment. In their application, a cancer cell line would be endowed with the capacity to metabolize cellobiose and then engrafted as tumors. After in vivo provision of isotopically labelled cellobiose, the tumors would metabolize the cellobiose and then excrete various metabolites that are labelled with heavy carbon. Next, TILs or any other cell of interest could be isolated from the tumor and the heavy carbon metabolite profile within the TILs assessed. For example, it would be interesting to assess the dynamic of lactate in this system, as the accumulation of lactic acid in the tumor environment has historically been associated with TIL suppression[92,93,104,187–191], but a large body of recent work has demonstrated that lactate can serve as an important fuel source for various tissues[192,193], including in activated T cells[10,171,194–196]. This strategy would provide a new tool in the study of tumor associated metabolites and their impact on TILs. It should be noted that isotopically labelled

glucose is less useful in the pursuit of dissecting tumor metabolic crosstalk, due to the inability to determine in which cell type the glucose was originally metabolized.

The cellobiose system is an interesting tool first developed for the production of biofuels, where it was introduced into industrially controlled microbes to facilitate the breakdown of lignocellulosic material[122]. In 2022, Teixeira et al. were the first group to introduce cellobiose catabolism into mammalian systems, where they applied the Celloselect system to generate a cell line that could be enriched for a GOI without the use of antibiotics or fluorophores[147]. Here, we have further developed the cellobiose system by introducing it for the first time into mammalian, primary cells, where we have applied the ability to metabolize cellobiose as a tool to exclusively fuel TILs, emboldening them as they participate in the battle between the immune cells and cancer. There is much work left to be done to optimize the system and to demonstrate more wide-spread utility across tumor types, but this work has laid the foundation for the application of cellobiose metabolism as a tool in cancer immunotherapy.

BIBLIOGRAPHY

1. Aktipis, C. A. *et al.* Cancer across the tree of life: cooperation and cheating in multicellularity. *Philosophical Transactions of the Royal Society B: Biological Sciences* **370**, 20140219 (2015).
2. Hanahan, D. & Weinberg, R. A. Hallmarks of Cancer: The Next Generation. *Cell* **144**, 646–674 (2011).
3. Mendiratta, G. *et al.* Cancer gene mutation frequencies for the U.S. population. *Nat Commun* **12**, 5961 (2021).
4. Schwartzenberg-Bar-Yoseph, F., Armoni, M. & Karnieli, E. The Tumor Suppressor p53 Down-Regulates Glucose Transporters GLUT1 and GLUT4 Gene Expression. *Cancer Research* **64**, 2627–2633 (2004).
5. Kondoh, H. *et al.* Glycolytic Enzymes Can Modulate Cellular Life Span. *Cancer Research* **65**, 177–185 (2005).
6. Bensaad, K. *et al.* TIGAR, a p53-Inducible Regulator of Glycolysis and Apoptosis. *Cell* **126**, 107–120 (2006).
7. Warburg, O. The Metabolism of Carcinoma Cells1. *The Journal of Cancer Research* **9**, 148–163 (1925).
8. Crabtree, H. G. Observations on the carbohydrate metabolism of tumours. *Biochemical Journal* **23**, 536–545 (1929).
9. Romano, A. H. & Conway, T. Evolution of carbohydrate metabolic pathways. *Research in Microbiology* **147**, 448–455 (1996).
10. Rabinowitz, J. D. & Enerbäck, S. Lactate: the ugly duckling of energy metabolism. *Nature Metabolism* **2**, 566–571 (2020).
11. Glycolysis. *Wikipedia* (2023).
12. Kilburn, D. G., Lilly, M. D. & Webb, F. C. The energetics of mammalian cell growth. *Journal of Cell Science* **4**, 645–654 (1969).

13. Scholnick, P., Lang, D. & Racker, E. Regulatory Mechanisms in Carbohydrate Metabolism: IX. STIMULATION OF AEROBIC GLYCOLYSIS BY ENERGY-LINKED ION TRANSPORT AND INHIBITION BY DEXTRAN SULFATE. *Journal of Biological Chemistry* **248**, 5175–5182 (1973).

14. Tanner, L. B. *et al.* Four Key Steps Control Glycolytic Flux in Mammalian Cells. *Cell Syst* **7**, 49-62.e8 (2018).

15. Shim, H. *et al.* c-Myc transactivation of LDH-A: Implications for tumor metabolism and growth. *Proceedings of the National Academy of Sciences* **94**, 6658–6663 (1997).

16. Kim, J., Gao, P., Liu, Y.-C., Semenza, G. L. & Dang, C. V. Hypoxia-Inducible Factor 1 and Dysregulated c-Myc Cooperatively Induce Vascular Endothelial Growth Factor and Metabolic Switches Hexokinase 2 and Pyruvate Dehydrogenase Kinase 1. *Molecular and Cellular Biology* **27**, 7381–7393 (2007).

17. Dang, C. V., Kim, J., Gao, P. & Yustein, J. The interplay between MYC and HIF in cancer. *Nat Rev Cancer* **8**, 51–56 (2008).

18. DeBerardinis, R. J. *et al.* Beyond aerobic glycolysis: Transformed cells can engage in glutamine metabolism that exceeds the requirement for protein and nucleotide synthesis. *Proceedings of the National Academy of Sciences* **104**, 19345–19350 (2007).

19. C, N. F. Chemical composition of Escherichia coli. *Esr^herichia coli and Salmonella: cellular and molecular biology* 13–16 (1996).

20. Jiang, P., Du, W. & Wu, M. Regulation of the pentose phosphate pathway in cancer. *Protein & Cell* **5**, 592–602 (2014).

21. Lunt, S. Y. & Vander Heiden, M. G. Aerobic glycolysis: Meeting the metabolic requirements of cell proliferation. *Annual Review of Cell and Developmental Biology* **27**, 441–464 (2011).

22. Chambers, D. A., Martin, D. W. & Weinstein, Y. The effect of cyclic nucleotides on purine biosynthesis and the induction of PRPP synthetase during lymphocyte activation. *Cell* **3**, 375–380 (1974).

23. Alberts, B. *Molecular Biology of the Cell*. (Garland Science, 2017).

24. Masui, K. *et al.* Glucose-dependent acetylation of Rictor promotes targeted cancer therapy resistance. *Proceedings of the National Academy of Sciences* **112**, 9406–9411 (2015).

25. Srere, P. A. The Molecular Physiology of Citrate. *Nature* **205**, 766–770 (1965).

26. Newsholme, E. A., Crabtree, B. & Ardawi, M. S. M. The role of high rates of glycolysis and glutamine utilization in rapidly dividing cells. *Biosci Rep* **5**, 393–400 (1985).

27. Schnaar, R. L., Sandhoff, R., Tiemeyer, M. & Kinoshita, T. Glycosphingolipids. in *Essentials of Glycobiology* (eds. Varki, A. et al.) (Cold Spring Harbor Laboratory Press, 2022).

28. Ferris, S. P., Kodali, V. K. & Kaufman, R. J. Glycoprotein folding and quality-control mechanisms in protein-folding diseases. *Dis Model Mech* **7**, 331–341 (2014).

29. Varki, A. Biological roles of glycans. *Glycobiology* **27**, 3–49 (2017).

30. Macheda, M. L., Rogers, S. & Best, J. D. Molecular and cellular regulation of glucose transporter (GLUT) proteins in cancer. *Journal of Cellular Physiology* **202**, 654–662 (2005).

31. Klip, A., McGraw, T. E. & James, D. E. Thirty sweet years of GLUT4. *J Biol Chem* **294**, 11369–11381 (2019).

32. Sun, L., Shukair, S., Naik, T. J., Moazed, F. & Ardehali, H. Glucose Phosphorylation and Mitochondrial Binding Are Required for the Protective Effects of Hexokinases I and II. *Molecular and Cellular Biology* **28**, 1007 (2008).

33. Maxwell, P. H. & Ratcliffe, P. J. Oxygen sensors and angiogenesis. *Seminars in Cell & Developmental Biology* **13**, 29–37 (2002).

34. Fraisl, P., Mazzone, M., Schmidt, T. & Carmeliet, P. Regulation of angiogenesis by oxygen and metabolism. *Dev Cell* **16**, 167–179 (2009).

35. Chen, C., Pore, N., Behrooz, A., Ismail-Beigi, F. & Maity, A. Regulation of glut1 mRNA by Hypoxia-inducible Factor-1: INTERACTION BETWEEN H-ras AND HYPOXIA *. *Journal of Biological Chemistry* **276**, 9519–9525 (2001).

36. Sakagami, H. *et al.* Loss of HIF-1α impairs GLUT4 translocation and glucose uptake by the skeletal muscle cells. *American Journal of Physiology-Endocrinology and Metabolism* **306**, E1065–E1076 (2014).

37. Denko, N. C. Hypoxia, HIF1 and glucose metabolism in the solid tumour. *Nat Rev Cancer* **8**, 705–713 (2008).

38. Firth, J. D., Ebert, B. L. & Ratcliffe, P. J. Hypoxic Regulation of Lactate Dehydrogenase A: INTERACTION BETWEEN HYPOXIA-INDUCIBLE FACTOR 1 AND cAMP RESPONSE ELEMENTS (∗). *Journal of Biological Chemistry* **270**, 21021–21027 (1995).

39. Ullah, M. S., Davies, A. J. & Halestrap, A. P. The Plasma Membrane Lactate Transporter MCT4, but Not MCT1, Is Up-regulated by Hypoxia through a HIF-1α-dependent Mechanism *. *Journal of Biological Chemistry* **281**, 9030–9037 (2006).

40. Kim, J. W., Tchernyshyov, I., Semenza, G. L. & Dang, C. V. HIF-1-mediated expression of pyruvate dehydrogenase kinase: A metabolic switch required for cellular adaptation to hypoxia. *Cell Metabolism* **3**, 177–185 (2006).

41. Papandreou, I., Cairns, R. A., Fontana, L., Lim, A. L. & Denko, N. C. HIF-1 mediates adaptation to hypoxia by actively downregulating mitochondrial oxygen consumption. *Cell Metabolism* **3**, 187–197 (2006).

42. Saharinen, P., Eklund, L., Pulkki, K., Bono, P. & Alitalo, K. VEGF and angiopoietin signaling in tumor angiogenesis and metastasis. *Trends in Molecular Medicine* **17**, 347–362 (2011).

43. Park, J.-S. *et al.* Normalization of Tumor Vessels by Tie2 Activation and Ang2 Inhibition Enhances Drug Delivery and Produces a Favorable Tumor Microenvironment. *Cancer Cell* **30**, 953–967 (2016).

44. Rezaei, M. *et al.* Interplay between neural-cadherin and vascular endothelial-cadherin in breast cancer progression. *Breast Cancer Research* **14**, R154 (2012).

45. Sun, R., Kong, X., Qiu, X., Huang, C. & Wong, P.-P. The Emerging Roles of Pericytes in Modulating Tumor Microenvironment. *Frontiers in Cell and Developmental Biology* **9**, (2021).

46. Barlow, K. D., Sanders, A. M., Soker, S., Ergun, S. & Metheny-Barlow, L. J. Pericytes on the Tumor Vasculature: Jekyll or Hyde? *Cancer Microenviron* **6**, 1–17 (2012).

47. Wen, H. Y., Abbasi, S., Kellems, R. E. & Xia, Y. mTOR: A placental growth signaling sensor. *Placenta* **26**, S63–S69 (2005).

48. Howell, J. J. & Manning, B. D. mTOR couples cellular nutrient sensing to organismal metabolic homeostasis. *Trends in Endocrinology & Metabolism* **22**, 94–102 (2011).

49. Han, J. *et al.* Glucose promotes cell proliferation, glucose uptake and invasion in endometrial cancer cells via AMPK/mTOR/S6 and MAPK signaling. *Gynecologic Oncology* **138**, 668–675 (2015).

50. Leprivier, G. & Rotblat, B. How does mTOR sense glucose starvation? AMPK is the usual suspect. *Cell Death Discov.* **6**, 1–5 (2020).

51. Ayala, J. E. *et al.* Standard operating procedures for describing and performing metabolic tests of glucose homeostasis in mice. *Dis Model Mech* **3**, 525–534 (2010).

52. Nakrani, M. N., Wineland, R. H. & Anjum, F. Physiology, Glucose Metabolism. in *StatPearls* (StatPearls Publishing, 2023).

53. Thennadil, S. N. *et al.* Comparison of Glucose Concentration in Interstitial Fluid, and Capillary and Venous Blood During Rapid Changes in Blood Glucose Levels. *Diabetes Technology & Therapeutics* **3**, 357–365 (2001).

54. Hirayama, A. *et al.* Quantitative metabolome profiling of colon and stomach cancer microenvironment by capillary electrophoresis time-of-flight mass spectrometry. *Cancer Research* **69**, 4918–4925 (2009).

55. Ho, P. C. *et al.* Phosphoenolpyruvate Is a Metabolic Checkpoint of Anti-tumor T Cell Responses. *Cell* **162**, 1217–1228 (2015).

56. Zhang, Y. *et al.* Enhancing CD8+ T Cell Fatty Acid Catabolism within a Metabolically Challenging Tumor Microenvironment Increases the Efficacy of Melanoma Immunotherapy. *Cancer Cell* **32**, 377-391.e9 (2017).

57. Tomasetti, C. & Vogelstein, B. Variation in cancer risk among tissues can be explained by the number of stem cell divisions. *Science* **347**, 78–81 (2015).

58. Tomlinson, I. P. M., Novelli, M. R. & Bodmer, W. F. The mutation rate and cancer. *Proceedings of the National Academy of Sciences* **93**, 14800–14803 (1996).

59. Jackson, A. L. & Loeb, L. A. The Mutation Rate and Cancer. *Genetics* **148**, 1483–1490 (1998).

60. Ehrlich: Ueber den jetzigen Stand der Karzinomforschung - Google Scholar. https://scholar.google.com/scholar_lookup?&title=Ueber%20den%20jetzigen%20stand%20der%20Karzinomforschung&journal=Ned.%20Tijdschr.%20Geneeskd.&volume=5&pages=273-290&publication_year=1909&author=Ehrlich%2CP.

61. Burnet, M. Cancer—A Biological Approach. *Br Med J* **1**, 841–847 (1957).

62. Burnet, F. M. The Concept of Immunological Surveillance. (1970) doi:10.1159/000386035.

63. van den Broek, M. E. *et al.* Decreased tumor surveillance in perforin-deficient mice. *Journal of Experimental Medicine* **184**, 1781–1790 (1996).

64. Smyth, M. J. *et al.* Perforin-Mediated Cytotoxicity Is Critical for Surveillance of Spontaneous Lymphoma. *Journal of Experimental Medicine* **192**, 755–760 (2000).

65. Smyth, M. J. *et al.* Differential Tumor Surveillance by Natural Killer (Nk) and Nkt Cells. *Journal of Experimental Medicine* **191**, 661–668 (2000).

66. Street, S. E. A., Cretney, E. & Smyth, M. J. Perforin and interferon-γ activities independently control tumor initiation, growth, and metastasis. *Blood* **97**, 192–197 (2001).

67. Shinkai, Y. *et al.* RAG-2-deficient mice lack mature lymphocytes owing to inability to initiate V(D)J rearrangement. *Cell* **68**, 855–867 (1992).

68. Shankaran, V. *et al.* IFNγ and lymphocytes prevent primary tumour development and shape tumour immunogenicity. *Nature* **410**, 1107–1111 (2001).

69. Pagès, F. *et al.* Immune infiltration in human tumors: a prognostic factor that should not be ignored. *Oncogene* **29**, 1093–1102 (2010).

70. Jochems, C. & Schlom, J. Tumor-infiltrating immune cells and prognosis: the potential link between conventional cancer therapy and immunity. *Experimental biology and medicine (Maywood, N.J.)* **236**, 567–79 (2011).

71. Naito, Y. *et al.* CD8+ T Cells Infiltrated within Cancer Cell Nests as a Prognostic Factor in Human Colorectal Cancer. *Cancer Research* **58**, 3491–3494 (1998).

72. Ovarian Tumor Tissue Analysis (OTTA) Consortium. Dose-Response Association of CD8+ Tumor-Infiltrating Lymphocytes and Survival Time in High-Grade Serous Ovarian Cancer. *JAMA Oncology* **3**, e173290 (2017).

73. Shimizu, S. *et al.* Tumor-infiltrating CD8+ T-cell density is an independent prognostic marker for oral squamous cell carcinoma. *Cancer Medicine* **8**, 80–93 (2019).

74. Guo, N. *et al.* CD8 + T cell infiltration is associated with improved survival and negatively correlates with hypoxia in clear cell ovarian cancer. *Sci Rep* **13**, 6530 (2023).

75. Smith, C. C. *et al.* Alternative tumour-specific antigens. *Nat Rev Cancer* **19**, 465–478 (2019).

76. Xie, N. *et al.* Neoantigens: promising targets for cancer therapy. *Sig Transduct Target Ther* **8**, 1–38 (2023).

77. MacIver, N. J., Michalek, R. D. & Rathmell, J. C. Metabolic Regulation of T Lymphocytes. *Annual Review of Immunology* **31**, 259–283 (2013).

78. Lindsten, T., June, C. H. & Thompson, C. B. Multiple mechanisms regulate c-myc gene expression during normal T cell activation. *The EMBO Journal* **7**, 2787–2794 (1988).

79. Wang, R. *et al.* The Transcription Factor Myc Controls Metabolic Reprogramming upon T Lymphocyte Activation. *Immunity* **35**, 871–882 (2011).

80. Menk, A. V. *et al.* Early TCR Signaling Induces Rapid Aerobic Glycolysis Enabling Distinct Acute T Cell Effector Functions. *Cell Reports* **22**, 1509–1521 (2018).

81. Zheng, Y., Delgoffe, G. M., Meyer, C. F., Chan, W. & Powell, J. D. Anergic T Cells Are Metabolically Anergic1. *The Journal of Immunology* **183**, 6095–6101 (2009).

82. Jacobs, S. R. *et al.* Glucose Uptake Is Limiting in T Cell Activation and Requires CD28-Mediated Akt-Dependent and Independent Pathways1. *The Journal of Immunology* **180**, 4476–4486 (2008).

83. Frauwirth, K. A. *et al.* The CD28 signaling pathway regulates glucose metabolism. *Immunity* **16**, 769–777 (2002).

84. Choi, B. K. *et al.* 4-1BB signaling activates glucose and fatty acid metabolism to enhance CD8+ T cell proliferation. *Cell Mol Immunol* **14**, 748–757 (2017).

85. Macintyre, A. N. *et al.* Protein kinase B controls transcriptional programs that direct cytotoxic T cell fate but is dispensable for T cell metabolism. *Immunity* **34**, 224–236 (2011).

86. Brennan, P. *et al.* Phosphatidylinositol 3-Kinase Couples the Interleukin-2 Receptor to the Cell Cycle Regulator E2F. *Immunity* **7**, 679–689 (1997).

87. Preston, G. C. *et al.* Single cell tuning of Myc expression by antigen receptor signal strength and interleukin-2 in T lymphocytes. *The EMBO Journal* **34**, 2008–2024 (2015).

88. Finlay, D. K. *et al.* PDK1 regulation of mTOR and hypoxia-inducible factor 1 integrate metabolism and migration of CD8+ T cells. *Journal of Experimental Medicine* **209**, 2441–2453 (2012).

89. Chang, C.-H. *et al.* Posttranscriptional Control of T Cell Effector Function by Aerobic Glycolysis. *Cell* **153**, 1239–1251 (2013).

90. Peng, M. *et al.* Aerobic glycolysis promotes T helper 1 cell differentiation through an epigenetic mechanism. *Science* **1002967**, aaf6284 (2016).

91. Dunn, G. P., Bruce, A. T., Ikeda, H., Old, L. J. & Schreiber, R. D. Cancer immunoediting: from immunosurveillance to tumor escape. *Nat Immunol* **3**, 991–998 (2002).

92. Fischer, K. *et al.* Inhibitory effect of tumor cell-derived lactic acid on human T cells. *Blood* **109**, 3812–9 (2007).

93. Brand, A. *et al.* LDHA-Associated Lactic Acid Production Blunts Tumor Immunosurveillance by T and NK Cells. *Cell Metabolism* **24**, 657–671 (2016).

94. Prendergast, G. C. Immune escape as a fundamental trait of cancer: focus on IDO. *Oncogene* **27**, 3889–3900 (2008).

95. MacIver, N. J. *et al.* Glucose metabolism in lymphocytes is a regulated process with significant effects on immune cell function and survival. *Journal of Leukocyte Biology* **84**, 949–957 (2008).

96. Brand, K. Glutamine and glucose metabolism during thymocyte proliferation. Pathways of glutamine and glutamate metabolism. *Biochemical Journal* **228**, 353–361 (1985).

97. Cham, C. M. & Gajewski, T. F. Glucose Availability Regulates IFN-γ Production and p70S6 Kinase Activation in CD8+ Effector T Cells1. *The Journal of Immunology* **174**, 4670–4677 (2005).

98. Cham, C. M., Driessens, G., O'Keefe, J. P. & Gajewski, T. F. Glucose deprivation inhibits multiple key gene expression events and effector functions in CD8+ T cells. *European Journal of Immunology* **38**, 2438–2450 (2008).

99. Blagih, J. *et al.* The energy sensor AMPK regulates T cell metabolic adaptation and effector responses in vivo. *Immunity* **42**, 41–54 (2015).

100. Hukelmann, J. L. *et al.* The cytotoxic T cell proteome and its shaping by the kinase mTOR. *Nat Immunol* **17**, 104–112 (2016).

101. Zhu, J. *et al.* High Glucose Enhances Cytotoxic T Lymphocyte-Mediated Cytotoxicity. *Frontiers in Immunology* **12**, (2021).

102. Klein Geltink, R. I. *et al.* Metabolic conditioning of CD8+ effector T cells for adoptive cell therapy. *Nat Metab* **2**, 703–716 (2020).

103. Chang, C.-H. *et al.* Metabolic Competition in the Tumor Microenvironment Is a Driver of Cancer Progression. *Cell* **162**, (2015).

104. Renner, K. *et al.* Restricting Glycolysis Preserves T Cell Effector Functions and Augments Checkpoint Therapy. *Cell Reports* **29**, 135-150.e9 (2019).

105. Singer, K. *et al.* Warburg phenotype in renal cell carcinoma: High expression of glucose-transporter 1 (GLUT-1) correlates with low CD8+ T-cell infiltration in the tumor. *International Journal of Cancer* **128**, 2085–2095 (2011).

106. Takahashi, H. *et al.* Upregulated glycolysis correlates with tumor progression and immune evasion in head and neck squamous cell carcinoma. *Sci Rep* **11**, 17789 (2021).

107. Cascone, T. *et al.* Increased Tumor Glycolysis Characterizes Immune Resistance to Adoptive T Cell Therapy. *Cell Metabolism* **27**, 977-987.e4 (2018).

108. Klemm, D., Heublein, B., Fink, H.-P. & Bohn, A. Cellulose: Fascinating Biopolymer and Sustainable Raw Material. *Angewandte Chemie International Edition* **44**, 3358–3393 (2005).

109. Vanderghem, C., Boquel, P., Blecker, C. & Paquot, M. A Multistage Process to Enhance Cellobiose Production from Cellulosic Materials. *Appl Biochem Biotechnol* **160**, 2300–2307 (2010).

110. Henriksson, G., Johansson, G. & Pettersson, G. A critical review of cellobiose dehydrogenases. *Journal of Biotechnology* **78**, 93–113 (2000).

111. Peña, L. *et al.* Cellobiose hydrolysis using acid-functionalized nanoparticles. *Biotechnol Bioproc E* **16**, 1214–1222 (2011).

112. Herr, D. Secretion of cellulase and β-glucosidase by Trichoderma viride ITCC-1433 in submerged culture on different substrates. *Biotechnology and Bioengineering* **21**, 1361–1371 (1979).

113. Tian, C. *et al.* Systems analysis of plant cell wall degradation by the model filamentous fungus Neurospora crassa. *Proceedings of the National Academy of Sciences* **106**, 22157–22162 (2009).

114. Weimer, P. J., Russell, J. B. & Muck, R. E. Lessons from the cow: What the ruminant animal can teach us about consolidated bioprocessing of cellulosic biomass. *Bioresource Technology* **100**, 5323–5331 (2009).

115. Nakamura, S., Oku, T. & Ichinose, M. Bioavailability of cellobiose by tolerance test and breath hydrogen excretion in humans. *Nutrition* **20**, 979–983 (2004).

116. Ocasio-Vega, C. *et al.* Effect of cellobiose supplementation and dietary soluble fibre content on in vitro caecal fermentation of carbohydrate-rich substrates in rabbits. *Archives of Animal Nutrition* **72**, 221–238 (2018).

117. Moré, M. I., Postrach, E., Bothe, G., Heinritz, S. & Uebelhack, R. A Dose-Escalation Study Demonstrates the Safety and Tolerability of Cellobiose in Healthy Subjects. *Nutrients* **12**, 64 (2019).

118. Andersen, D. W., Daabees, T. T., Applebaum, A. E., Filer, L. J. & Stegink, L. D. Utilization of intravenously administered β-cellobiose and maltose by young pigs. *Journal of Nutrition* **113**, 1039–1045 (1983).

119. Cobden, I., Hamilton, I., Rothwell, J. & Axon, A. T. R. Cellobiose/mannitol test: physiological properties of probe molecules and influence of extraneous factors. *Clinica Chimica Acta* **148**, 53–62 (1985).

120. Tseng, W.-C., Tang, C.-H., Fang, T.-Y. & Su, L.-Y. Using disaccharides to enhance in vitro and in vivo transgene expression mediated by a lipid-based gene delivery system. *The Journal of Gene Medicine* **9**, 659–667 (2007).

121. Chomvong, K. *et al.* Overcoming inefficient cellobiose fermentation by cellobiose phosphorylase in the presence of xylose. *Biotechnology for Biofuels* **7**, 85 (2014).

122. Galazka, J. M. *et al.* Cellodextrin transport in yeast for improved biofuel production. *Science* **330**, 84–86 (2010).

123. Ha, S.-J. *et al.* Engineered Saccharomyces cerevisiae capable of simultaneous cellobiose and xylose fermentation. *Proceedings of the National Academy of Sciences of the United States of America* **108**, 504–9 (2011).

124. Oh, E. J. *et al.* Enhanced xylitol production through simultaneous co-utilization of cellobiose and xylose by engineered Saccharomyces cerevisiae. *Metabolic Engineering* **15**, 226–234 (2013).

125. Kim, H., Lee, W.-H., Galazka, J. M., Cate, J. H. D. & Jin, Y.-S. Analysis of cellodextrin transporters from Neurospora crassa in Saccharomyces cerevisiae for cellobiose fermentation. *Applied Microbiology and Biotechnology* **98**, 1087–1094 (2014).

126. Hu, M.-L. *et al.* Enhanced Bioconversion of Cellobiose by Industrial Saccharomyces cerevisiae Used for Cellulose Utilization. *Frontiers in Microbiology* **7**, (2016).

127. Kim, H. *et al.* Enhanced cellobiose fermentation by engineered Saccharomyces cerevisiae expressing a mutant cellodextrin facilitator and cellobiose phosphorylase. *Journal of Biotechnology* **275**, 53–59 (2018).

128. Cai, P. *et al.* Evidence of a Critical Role for Cellodextrin Transporte 2 (CDT-2) in Both Cellulose and Hemicellulose Degradation and Utilization in Neurospora crassa. *PLOS ONE* **9**, e89330 (2014).

129. Ha, S. J. *et al.* Energetic benefits and rapid cellobiose fermentation by Saccharomyces cerevisiae expressing cellobiose phosphorylase and mutant cellodextrin transporters. *Metabolic Engineering* **15**, 134–143 (2013).

130. Lian, J., Li, Y., Hamedirad, M. & Zhao, H. Directed Evolution of a Cellodextrin Transporter for Improved Biofuel Production Under Anaerobic Conditions in Saccharomyces cerevisiae. *Biotechnol. Bioeng* **111**, 1521–1531 (2014).

131. Koning, S. M., Elferink, M. G. L., Konings, W. N. & Driessen, A. J. M. Cellobiose Uptake in the Hyperthermophilic ArchaeonPyrococcus furiosus Is Mediated by an Inducible, High-Affinity ABC Transporter. *Journal of Bacteriology* **183**, 4979–4984 (2001).

132. Bae, Y.-H., Kang, K.-H., Jin, Y.-S. & Seo, J.-H. Molecular cloning and expression of fungal cellobiose transporters and β-glucosidases conferring efficient cellobiose fermentation in Saccharomyces cerevisiae. *Journal of Biotechnology* **169**, 34–41 (2014).

133. dos Reis, T. F. *et al.* Identification and characterization of putative xylose and cellobiose transporters in Aspergillus nidulans. *Biotechnology for Biofuels* **9**, 204 (2016).

134. Guedon, E., Payot, S., Desvaux, M. & Petitdemange, H. Relationships between cellobiose catabolism, enzyme levels, and metabolic intermediates in Clostridium cellulolyticum grown in a synthetic medium. *Biotechnology and Bioengineering* **67**, 327–335 (2000).

135. Zha, J. *et al.* Optimization of CDT-1 and XYL1 Expression for Balanced Co-Production of Ethanol and Xylitol from Cellobiose and Xylose by Engineered Saccharomyces cerevisiae. *PLOS ONE* **8**, e68317 (2013).

136. Oh, E. J. *et al.* Gene Amplification on Demand Accelerates Cellobiose Utilization in Engineered Saccharomyces cerevisiae. *Applied and Environmental Microbiology* **82**, 3631–3639 (2016).

137. Fu, H. *et al.* Codon optimization with deep learning to enhance protein expression. *Sci Rep* **10**, 17617 (2020).

138. Bantug, G. R., Galluzzi, L., Kroemer, G. & Hess, C. The spectrum of T cell metabolism in health and disease. *Nature Reviews Immunology* **18**, 19–34 (2017).

139. Geltink, R. I. K., Kyle, R. L. & Pearce, E. L. Unraveling the Complex Interplay between T Cell Metabolism and Function. *Annual Review of Immunology* **36**, 461–488 (2018).

140. Ma, E. H. *et al.* Metabolic Profiling Using Stable Isotope Tracing Reveals Distinct Patterns of Glucose Utilization by Physiologically Activated CD8+ T Cells. *Immunity* **51**, 856-870.e5 (2019).

141. Palmer, C. S., Ostrowski, M., Balderson, B., Christian, N. & Crowe, S. M. Glucose Metabolism Regulates T Cell Activation, Differentiation, and Functions. *Frontiers in Immunology* **6**, (2015).

142. Rolf, J. *et al.* AMPKα1: A glucose sensor that controls CD8 T-cell memory. *European Journal of Immunology* **43**, 889–896 (2013).

143. Chang, C. H. *et al.* Metabolic Competition in the Tumor Microenvironment Is a Driver of Cancer Progression. *Cell* **162**, 1229–1241 (2015).

144. Lambertz, C. *et al.* Challenges and advances in the heterologous expression of cellulolytic enzymes: A review. *Biotechnology for Biofuels* **7**, 135 (2014).

145. Bischof, R. H., Ramoni, J. & Seiboth, B. Cellulases and beyond: The first 70 years of the enzyme producer Trichoderma reesei. *Microbial Cell Factories* **15**, (2016).

146. Jang, S. *et al.* Glycolytic enzymes localize to synapses under energy stress to support synaptic function. *Neuron* **90**, 278–291 (2016).

147. Teixeira, A. P. *et al.* CelloSelect – A synthetic cellobiose metabolic pathway for selection of stable transgenic CHO cell lines. *Metabolic Engineering* **70**, 23–30 (2022).

148. Ha, S. J. *et al.* Energetic benefits and rapid cellobiose fermentation by Saccharomyces cerevisiae expressing cellobiose phosphorylase and mutant cellodextrin transporters. *Metabolic Engineering* **15**, 134–143 (2013).

149. Gradinaru, V. *et al.* Molecular and Cellular Approaches for Diversifying and Extending Optogenetics. *Cell* **141**, 154–165 (2010).

150. Li, J. *et al.* Cellodextrin transporters play important roles in cellulase induction in the cellulolytic fungus Penicillium oxalicum. *Appl Microbiol Biotechnol* **97**, 10479–10488 (2013).

151. Lin, H. *et al.* Identification and Characterization of a Cellodextrin Transporter in Aspergillus niger. *Frontiers in Microbiology* **11**, (2020).

152. Davies, J. S. *et al.* Non-synergy of PD-1 blockade with T-cell therapy in solid tumors. *J Immunother Cancer* **10**, e004906 (2022).

153. Blank, C. & Mackensen, A. Contribution of the PD-L1/PD-1 pathway to T-cell exhaustion: an update on implications for chronic infections and tumor evasion. *Cancer Immunol Immunother* **56**, 739–745 (2007).

154. Ghoneim, H. E. *et al.* De Novo Epigenetic Programs Inhibit PD-1 Blockade-Mediated T Cell Rejuvenation. *Cell* **170**, 142-157.e19 (2017).

155. Pauken, K. E., Torchia, J. A., Chaudhri, A., Sharpe, A. H. & Freeman, G. J. Emerging concepts in PD-1 checkpoint biology. *Seminars in Immunology* **52**, 101480 (2021).

156. Chemnitz, J. M., Parry, R. V., Nichols, K. E., June, C. H. & Riley, J. L. SHP-1 and SHP-2 Associate with Immunoreceptor Tyrosine-Based Switch Motif of Programmed Death 1 upon Primary Human T Cell Stimulation, but Only Receptor Ligation Prevents T Cell Activation1. *The Journal of Immunology* **173**, 945–954 (2004).

157. Patsoukis, N. *et al.* PD-1 Induces Metabolic Reprogramming Of Activated T Cells From Glycolysis To Lipid Oxidation. *Blood* **122**, 187 (2013).

158. Kawasaki, Y. *et al.* Mesenchymal Stromal Cells Inhibit Aerobic Glycolysis in Activated T Cells by Negatively Regulating Hexokinase II Activity Through PD-1/PD-L1 Interaction. *Transplantation and Cellular Therapy* **27**, 231.e1-231.e8 (2021).

159. Bengsch, B. *et al.* Bioenergetic Insufficiencies Due to Metabolic Alterations Regulated by the Inhibitory Receptor PD-1 Are an Early Driver of CD8+ T Cell Exhaustion. *Immunity* **45**, 358–373 (2016).

160. Qorraj, M. *et al.* The PD-1/PD-L1 axis contributes to immune metabolic dysfunctions of monocytes in chronic lymphocytic leukemia. *Leukemia* **31**, 470–478 (2017).

161. Lu, L.-G. *et al.* PD-L1 blockade liberates intrinsic antitumourigenic properties of glycolytic macrophages in hepatocellular carcinoma. *Gut* **71**, 2551–2560 (2022).

162. Keir, M. E., Butte, M. J., Freeman, G. J. & Sharpe, A. H. PD-1 and Its Ligands in Tolerance and Immunity. *Annual Review of Immunology* **26**, 677–704 (2008).

163. Cha, J.-H., Chan, L.-C., Li, C.-W., Hsu, J. L. & Hung, M.-C. Mechanisms controlling PD-L1 expression in cancer. *Mol Cell* **76**, 359–370 (2019).

164. Zhao, Y. *et al.* Antigen-Presenting Cell-Intrinsic PD-1 Neutralizes PD-L1 in cis to Attenuate PD-1 Signaling in T Cells. *Cell Rep* **24**, 379-390.e6 (2018).

165. Roslin, M., Henriksson, R., Bergström, P., Ungerstedt, U. & Tommy Bergenheim, A. Baseline Levels of Glucose Metabolites, Glutamate and Glycerol in Malignant Glioma Assessed by Stereotactic Microdialysis. *J Neurooncol* **61**, 151–160 (2003).

166. Wiig, H., Aukland, K. & Tenstad, O. Isolation of interstitial fluid from rat mammary tumors by a centrifugation method. *https://doi.org/10.1152/ajpheart.00327.2002* **284**, (2003).

167. Haslene-Hox, H. *et al.* A New Method for Isolation of Interstitial Fluid from Human Solid Tumors Applied to Proteomic Analysis of Ovarian Carcinoma Tissue. *PLOS ONE* **6**, e19217 (2011).

168. Sullivan, M., Lewis, C. & Muir, A. Isolation and Quantification of Metabolite Levels in Murine Tumor Interstitial Fluid by LC/MS. *BIO-PROTOCOL* **9**, (2019).

169. Goveia, J. *et al.* Meta-analysis of clinical metabolic profiling studies in cancer: challenges and opportunities. *EMBO Molecular Medicine* **8**, 1134–1142 (2016).

170. Sullivan, M. R. *et al.* Quantification of microenvironmental metabolites in murine cancers reveals determinants of tumor nutrient availability. *eLife* **8**, (2019).

171. García-Canaveras, J. C., Chen, L. & Rabinowitz, J. D. The tumor metabolic microenvironment: Lessons from lactate. *Cancer Research* **79**, 3155–3162 (2019).

172. Siska, P. J. *et al.* Mitochondrial dysregulation and glycolytic insufficiency functionally impair CD8 T cells infiltrating human renal cell carcinoma. *JCI insight* **2**, (2017).

173. Liu, M.-X. *et al.* Metabolic reprogramming by PCK1 promotes TCA cataplerosis, oxidative stress and apoptosis in liver cancer cells and suppresses hepatocellular carcinoma. *Oncogene* **37**, 1637–1653 (2018).

174. Beckermann, K. E. *et al.* CD28 costimulation drives tumor-infiltrating T cell glycolysis to promote inflammation. *JCI Insight* **5**, (2020).

175. Reinfeld, B. I. *et al.* Cell-programmed nutrient partitioning in the tumour microenvironment. *Nature* **593**, 282–288 (2021).

176. Hensley, C. T. *et al.* Metabolic Heterogeneity in Human Lung Tumors. *Cell* **164**, 681–94 (2016).

177. Koh, D.-M. & Collins, D. J. Diffusion-weighted MRI in the body: applications and challenges in oncology. *AJR Am J Roentgenol* **188**, 1622–1635 (2007).

178. Fletcher, J. W. *et al.* Recommendations on the Use of 18F-FDG PET in Oncology. *Journal of Nuclear Medicine* **49**, 480–508 (2008).

179. Wagner, D. L. *et al.* Immunogenicity of CAR T cells in cancer therapy. *Nat Rev Clin Oncol* **18**, 379–393 (2021).

180. Wang, V., Gauthier, M., Decot, V., Reppel, L. & Bensoussan, D. Systematic Review on CAR-T Cell Clinical Trials Up to 2022: Academic Center Input. *Cancers (Basel)* **15**, 1003 (2023).

181. Gauthier, J. *et al.* Factors associated with outcomes after a second CD19-targeted CAR T-cell infusion for refractory B-cell malignancies. *Blood* **137**, 323–335 (2021).

182. Afshar, S., Asai, T. & Morrison, S. L. Humanized ADEPT Comprised of an Engineered Human Purine Nucleoside Phosphorylase and a Tumor Targeting Peptide for Treatment of Cancer. *Molecular cancer therapeutics* **8**, 185 (2009).

183. Wang, Y. *et al.* Directed Evolution: Methodologies and Applications. *Chem. Rev.* **121**, 12384–12444 (2021).

184. Larue, K., Melgar, M. & Martin, V. J. J. Directed evolution of a fungal β-glucosidase in Saccharomyces cerevisiae. *Biotechnol Biofuels* **9**, 52 (2016).

185. Li, H., Schmitz, O. & Alper, H. S. Enabling glucose/xylose co-transport in yeast through the directed evolution of a sugar transporter. *Appl Microbiol Biotechnol* **100**, 10215–10223 (2016).

186. Reinhart, D. *et al.* Bioprocessing of Recombinant CHO-K1, CHO-DG44, and CHO-S: CHO Expression Hosts Favor Either mAb Production or Biomass Synthesis. *Biotechnology Journal* **14**, 1700686 (2019).

187. Calcinotto, A. *et al.* Modulation of microenvironment acidity reverses anergy in human and murine tumor-infiltrating T lymphocytes. *Cancer research* **72**, 2746–56 (2012).

188. Mendler, A. N. *et al.* Tumor lactic acidosis suppresses CTL function by inhibition of p38 and JNK/c-Jun activation. *International Journal of Cancer* **131**, 633–640 (2012).

189. Schwickert, G., Walenta, S., Mueller-Klieser, W., Sundfør, K. & Rofstad, E. K. Correlation of High Lactate Levels in Human Cervical Cancer with Incidence of Metastasis. *Cancer Research* **55**, 4757–4759 (1995).

190. Angelin, A. *et al.* Foxp3 Reprograms T Cell Metabolism to Function in Low-Glucose, High-Lactate Environments. *Cell Metabolism* **25**, 1282-1293.e7 (2017).

191. Husain, Z., Huang, Y., Seth, P. & Sukhatme, V. P. Tumor-Derived Lactate Modifies Antitumor Immune Response: Effect on Myeloid-Derived Suppressor Cells and NK Cells. *The Journal of Immunology* **191**, 1486–1495 (2013).

192. Faubert, B. *et al.* Lactate Metabolism in Human Lung Tumors. *Cell* **171**, 358-371.e9 (2017).

193. Hui, S. *et al.* Glucose feeds the TCA cycle via circulating lactate. *Nature* **551**, 115–118 (2017).

194. Rundqvist, H. *et al.* Lactate Potentiates Differentiation and Expansion of Cytotoxic T Cells. *SSRN Electronic Journal* (2019) doi:10.2139/ssrn.3411249.

195. Feng, Q. *et al.* Lactate increases stemness of CD8 + T cells to augment anti-tumor immunity. *Nat Commun* **13**, 4981 (2022).

196. Kaymak, I. *et al.* Carbon source availability drives nutrient utilization in CD8+ T cells. *Cell Metab* **34**, 1298-1311.e6 (2022).